

DELAY TIME IN THE ALPHA TO  
GAMMA TRANSFORMATION OF IRON

Thesis by  
Olaf A. Boedtker

In Partial Fulfillment of the Requirements

For the Degree of  
Doctor of Philosophy

California Institute of Technology  
Pasadena, California

1961

ACKNOWLEDGEMENT

The author wishes to express his gratitude for the advice and encouragement given him by Professor Pol Duwez, as well as his suggestions in the preparation of this thesis. The author is also indebted to the members of the Physical Metallurgy Group of this Institute for many suggestions and technical assistance, without which this work would not have been possible.

The author is also very grateful to the Office of Naval Research for the substantial financial support over the entire period of this investigation.

ABSTRACT

Iron, containing a certain amount of carbon and nitrogen, was pulse-heated from an initial temperature in the alpha phase into a final temperature within the gamma phase. The bulk of the allotropic transformation took place a certain time after the final temperature had been reached. The relationship between this delay time and the final temperature follows an Arrhenius type rate equation with a heat of activation of  $20,500 \pm 1400$  cal per mole. It was also established that under the present experimental conditions alpha iron can be heated directly into the delta phase without going through the gamma phase. The effect of the rate of heating on the alpha to gamma transformation temperature can be deduced from the measurements of the delay time.

An interpretation of a possible transformation mechanism is given. It is assumed that the transformation takes place in two steps: (1) A relatively slow diffusion-like growth of nuclei of the new phase in the old matrix to their critical size, followed by (2) a very fast shear transformation.

TABLE OF CONTENTS

<u>PART</u>	<u>TITLE</u>	<u>PAGE</u>
	ACKNOWLEDGEMENTS . . . . .	i
	ABSTRACT . . . . .	ii
	LIST OF FIGURES . . . . .	iv
I.	INTRODUCTION . . . . .	1
II.	BACKGROUND DISCUSSION . . . . .	3
III.	EXPERIMENTAL METHODS . . . . .	8
	A. Specimen . . . . .	12
	B. Furnace . . . . .	14
	C. Temperature measurements . . . . .	23
	D. Rate of heating technique . . . . .	26
	E. Pulse heating technique . . . . .	29
IV.	EXPERIMENTAL RESULTS . . . . .	35
	A. Rate of heating experiments . . . . .	35
	B. Pulse heating experiments . . . . .	44
	C. Correlation between rate of heating and pulse heating experiments . . . . .	59
V.	DISCUSSION OF RESULTS . . . . .	66
VI.	CONCLUSIONS . . . . .	70
	A. Experimental facts . . . . .	70
	B. Interpretation . . . . .	71
	REFERENCES . . . . .	72

LIST OF FIGURES

<u>FIG. NO.</u>	<u>TITLE</u>	<u>PAGE</u>
1.	Schematic diagram of the experimental assembly . . .	9
2.	General view of the experimental assembly . . . . .	10
3.	Portion of the experimental assembly showing (from left to right): The electronic control panel, the glass vacuum chamber with the furnace inside, and a Miller recording oscillograph. In the foreground is a Tektronix oscilloscope . . . . .	11
4.	Sketch of the specimen with the attached thermocouple wires . . . . .	13
5.	Sketch of the spotwelding jig . . . . .	15
6.	Spotwelding jig and spotwelding power supply . . . . .	16
7.	Schematic cross-section of the furnace . . . . .	17
8.	Front view of the furnace . . . . .	19
9.	Temperature distribution along the specimen in the furnace under black body conditions . . . . .	20
10.	Temperature distribution along the specimen when the specimen is heated above the furnace temperature. . .	21
11.	Diagram showing the method to nullify potentials due to non thermal emf's along the specimen . . . . .	24
12.	Wiring diagram of the recording unit . . . . .	25
13.	Calibration curve relating the galvanometer deflection to the temperature. The insert in the figure shows the actual measurements obtained by various methods . . .	27
14.	Wiring diagram for calibrating the recording galvanometer . . . . .	28
15.	Circuit diagram of the pulse forming network . . . . .	30
16.	Shape of three voltage pulses showing different strength . . . . .	34
17.	Typical record of the temperature of the specimen versus time in a rate of heating experiment . . . . .	36

LIST OF FIGURES (continued)

<u>FIG. NO.</u>	<u>TITLE</u>	<u>PAGE</u>
18.	Typical record of a rate of heating experiment showing the graphical technique used for determining the rate of heating . . . . .	37
19.	Partial phase diagram of the iron-oxygen system . .	39
20.	Partial phase diagram of the iron-carbon system . .	40
21.	Partial phase diagram of the iron-nitrogen system . . . . .	41
22.	Typical records from rate of heating experiments initial temperature $T_i = 840$ C . . . . .	42
23.	Effect of the rate of heating on the alpha to gamma transformation temperature in iron for two different initial temperatures . . . . .	45
24.	Typical records from rate of heating experiments. Initial temperature $T_i = 880$ c . . . . .	46
25.	Typical records from pulse heating experiments. Initial temperature $T_i = 840$ C . . . . .	49
26.	Results of the pulse heating experiments showing the delay time for the alpha to gamma transformation at various temperatures . . . . .	54
27.	Typical records from pulse heating experiments. Initial temperature $T_i = 800$ C . . . . .	56
28.	Typical records from pulse heating experiments. Initial temperature $T_i = 880$ C . . . . .	57
29.	Results of pulse heating experiments (same as shown in Fig. 26) plotted on log of delay time versus reciprocal of absolute temperature scales . . . . .	58
30.	Typical record demonstrating passage from alpha to delta iron without transformation into the gamma phase . . . . .	60

LIST OF FIGURES (continued)

<u>FIG. NO.</u>	<u>TITLE</u>	<u>PAGE</u>
31.	Diagram demonstrating the method used for correlating the results of pulse heating and rate of heating experiments . . . . .	62
32.	Experimental curve of transformation temperature versus rate of heating (A) and calculated curve (B) deduced from the pulse heating experiments . . . . .	64

## 1 INTRODUCTION

An allotropic transformation in pure metals consists of a change in crystal structure. This change takes place at some critical values of temperature and pressure. Allotropic transformations exist in manganese, iron, cobalt, titanium, zirconium, hafnium, thorium, uranium, thallium, tin, calcium and some of the rare earth elements. For most of these elements (tin being an exception) and under atmospheric pressure the transformation occurs very rapidly within a very narrow range of temperatures. Many experimental evidences have been found to substantiate this statement. One of the simplest experiments consists of cooling a specimen very rapidly from the high temperature phase to the low temperature phase in an attempt to suppress the transformation. With the presently available cooling rates (of the order of 30,000 C per second) the high temperature phases of the metals listed above have never been completely retained at low temperature. The time required for a change of phase, however, must be finite. The new phase must nucleate within the matrix of the old one, it must grow (through a diffusion or a shear process), and the atomic motions involved in the transformation follow some kind of rate process. The main purpose of this thesis was to measure the time required for an allotropic transformation to proceed to completion. This time has been determined for the allotropic transformation in iron, from the alpha (low temperature) body-centered phase to the gamma (high temperature) face-centered phase. It has been shown that the time required to complete the transformation varies between 10 and 100 milliseconds,



depending on the temperature at which the transformation takes place. The analysis of the experimental results leads to the conclusion that the alpha to gamma transformation in iron occurs in two steps: first, nuclei of the new phase form and grow progressively until they reach a critical size; second, a rapid shear type atomic motion originates around the nuclei and very rapidly propagates into the entire volume of the specimen.

In interpreting the results described in this thesis, as well as the conclusions reached by the author, it should be borne in mind that the iron in this experimental study was not "pure iron". The word pure is, of course, relative and requires a quantitative explanation. Whereas in semi-conductors the purity is expressed in terms of  $10^{-12}$  parts per million, in metals which lend themselves to the purification techniques used for semi-conductors, the total purity content is of the order of 10 parts per million. This purity level can be obtained in relatively non-reactive metals, and elimination of non-metallic impurities (carbon, nitrogen, oxygen, etc.) is most difficult. At the onset of this research, unsuccessful attempts were made to procure a sufficient amount of pure iron refined by the zone floating technique, and the study was carried out using commercially available "spectroscopically pure" material with a total impurity concentration of carbon plus nitrogen of the order of 250 parts per million.

---

## II BACKGROUND DISCUSSION

The study of allotropic transformations in metals is but one part of a more general subject of phase transformations in multi-component alloys. Many theories of phase transformations have been advanced, and excellent reviews of the subject have been given by Tisza, (1) Seitz, (2) Smoluchowsky, (3) Barrett, (4) Meyer, (5) Cohen (6) and Hardy and Heal (7). For multicomponent transformations in which diffusion is the controlling factor, the theories have reached a high degree of reliability. The mechanism of precipitation from super-saturated solid solutions, for example, is well understood from both kinetics and crystallography standpoints. When a shear mechanism in addition to diffusion is involved in the transformation, the theories become more involved.

By far the greatest number of studies of this type of transformation have been concerned with the martensite reaction in steels. Several theories of this transformation have been proposed. In particular Cohen, (6,8,9,10) suggested that the reaction is nucleated by a strain embryo and the transformation proceeds as a plastic shear wave. Assuming that the strain embryo behaves like a screw dislocation, the crystallographic relationship between the martensite and the parent phase can be fairly well predicted. A more detailed dislocation mechanism of nucleation and propagation of a martensite transformation has been proposed by Jaswon (11). In other theories the martensite transformation is treated from the point of view of

nucleation and growth <sup>(12)</sup>. These theories also lead to the prediction of a crystallographic relationship, which is in general not the same as that predicted by the theory based on the existence of a strain embryo. Both kinds of theories cannot claim to be generally applicable and are valid in specific cases only.

The allotropic transformation mechanisms in most of the pure metals, and in particular in iron, is somewhat related to that of the martensite transformation in steel. Experimentally, the martensite transformation is probably easier to study than the transformation in iron, mostly because it can be stopped at various stages of completion, and both metallographic and x-ray diffraction technique can be used to follow the reaction. For pure iron, the interval of temperatures between the beginning and the end of the reaction is probably very small, and experiments of the type used for studying the martensite reaction are very difficult.

Actual visualization of the motion of the phase boundary between alpha and gamma iron during transformation has been recently obtained by Eichen and Spretnak <sup>(13)</sup>. These investigators have demonstrated that the boundary between the alpha and the gamma phases in high purity iron moves discontinuously. They interpret these results as proof for the existence of a martensitic type of transformation in pure iron.

Most of the evidence in favor of the concept of a very fast reaction rate for allotropic transformation in pure metals is based on results of experiments performed under conditions of fast cooling.

The early results of Esser et al <sup>(14)</sup> demonstrated that the gamma to alpha transformation in iron cannot be suppressed at cooling rates of the order of 10,000 C per second. In these experiments, it was also shown that the transformation temperature can be depressed from 905 C to about 500 C by increasing the rate of cooling. The only information on the carbon content in the iron used by Esser was that it was less than 170 parts per million (ppm), and no values were given for nitrogen, oxygen and metallic impurity contents. In 1951, Duwez <sup>(15)</sup> reinvestigated the effect of rapid cooling on the allotropic temperature of iron, using a technique developed by Greninger <sup>(16)</sup> for the study of the martensite reaction. The results of Esser were confirmed, although the drop in transformation temperature versus rate of cooling was less pronounced (740 C instead of 500 C at 10,000 C per second). The difference between the two sets of measurements is probably due to the effect of impurities on the kinetics of transformation. In addition to iron, the effect of rapid cooling was also studied on the transformation in titanium, zirconium, thallium, <sup>(15)</sup> hafnium, <sup>(17)</sup> and uranium <sup>(18)</sup>. These experimental results demonstrate that allotropic transformations in metals require some time to occur (which is a priori an obvious statement). However, they are not easy to interpret quantitatively. If, instead of the rate of cooling, the actual time it takes for the transformation to occur at a given temperature could be measured, interpretable data would be obtained. To establish a relationship between temperature and time, the specimen

should be cooled, or heated "instantaneously" from an initial temperature at which the other phase is stable. From the practical standpoint, the term instantaneously should be replaced by "fast enough" so that the time required to change the specimen temperature from the initial temperature to the final one is small with respect to the time required for the transformation to reach completion. Under such conditions, a meaningful value of the time required for complete transformation at a given temperature would be obtained.

The published results on the effect of the rate of cooling on the allotropic transformation of iron give some information on the order of magnitude of the time required for the change of phase. At a rate of cooling of 10,000 C per second, the transformation temperature from gamma to alpha iron is decreased by about 200 C. It may therefore be estimated that about 20 milliseconds are required for the transformation to be completed. Provided the temperature of the specimen can be changed from its initial value to its final value in microseconds, a quasi "instantaneous" temperature change could be assumed. Therefore, the main experimental problem is to apply to the specimen a temperature "pulse" in the microseconds range. Whether this temperature pulse results in cooling or heating the specimen is not important in principle. In both cases, useful information could be obtained on the kinetics of phase transformation. From a practical standpoint, however, rapid heating is much easier to achieve than rapid cooling. Cooling of a solid specimen is controlled by the rate of heat transfer to the surrounding medium and this imposes serious physical limitations. The fastest rates of cooling of a solid specimen so far reported are in the range of 10,000

to 50,000 C per second. On the other hand, rates of heating of the order of 5,000,000 C per second or more have been obtained by discharging electrical energy into specimens in the form of thin wires <sup>(19)</sup>. Realizing the obvious advantages of a heating technique over a cooling technique, the present study was limited to the kinetics of allotropic transformation from the low temperature (alpha) to the high temperature (gamma) phase of iron.

### III EXPERIMENTAL METHODS

The study of the kinetics of allotropic transformation from the alpha to the gamma phase in iron was approached from two different angles. First, the effect of the rate of heating on the alpha to gamma transformation temperature was determined. Second, the actual time it takes for the transformation to proceed to completion at various temperatures within the gamma range was measured.

All experiments were performed on iron wires 0.020 inch in diameter. The wire was placed along the axis of a cylindrical furnace located in a vacuum chamber. The furnace was then brought to an equilibrium temperature below the alpha to gamma transformation temperature. In a first series of experiments, referred to as "rate of heating experiments," the temperature of the specimen was raised at an approximately constant rate by applying a constant voltage across the wire. In a second series of experiments, referred to as "pulse heating experiments", the temperature of the specimen was rapidly increased from its initial temperature in the alpha field to a final temperature in the gamma field. This final temperature was maintained until the transformation was completed. To achieve this condition, the wire was heated by means of two voltage pulses, a first one of high voltage and short duration and a second one of low voltage and long duration.

The main components of the experimental assembly are shown diagrammatically in Fig. 1, and two views of the equipment are presented in Fig. 2 and 3, respectively. The most important components, namely

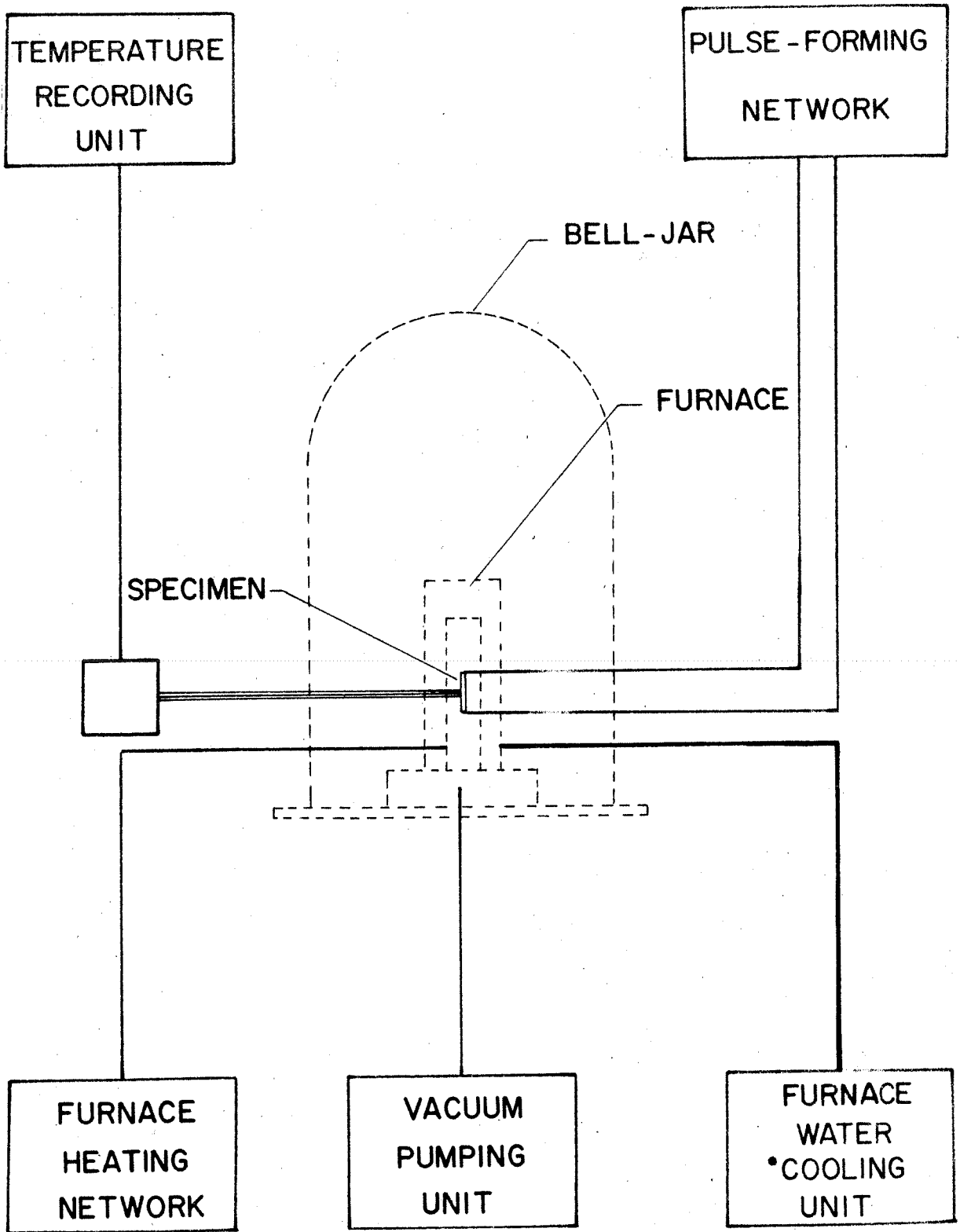


Fig. 1 - Schematic diagram of the experimental assembly.



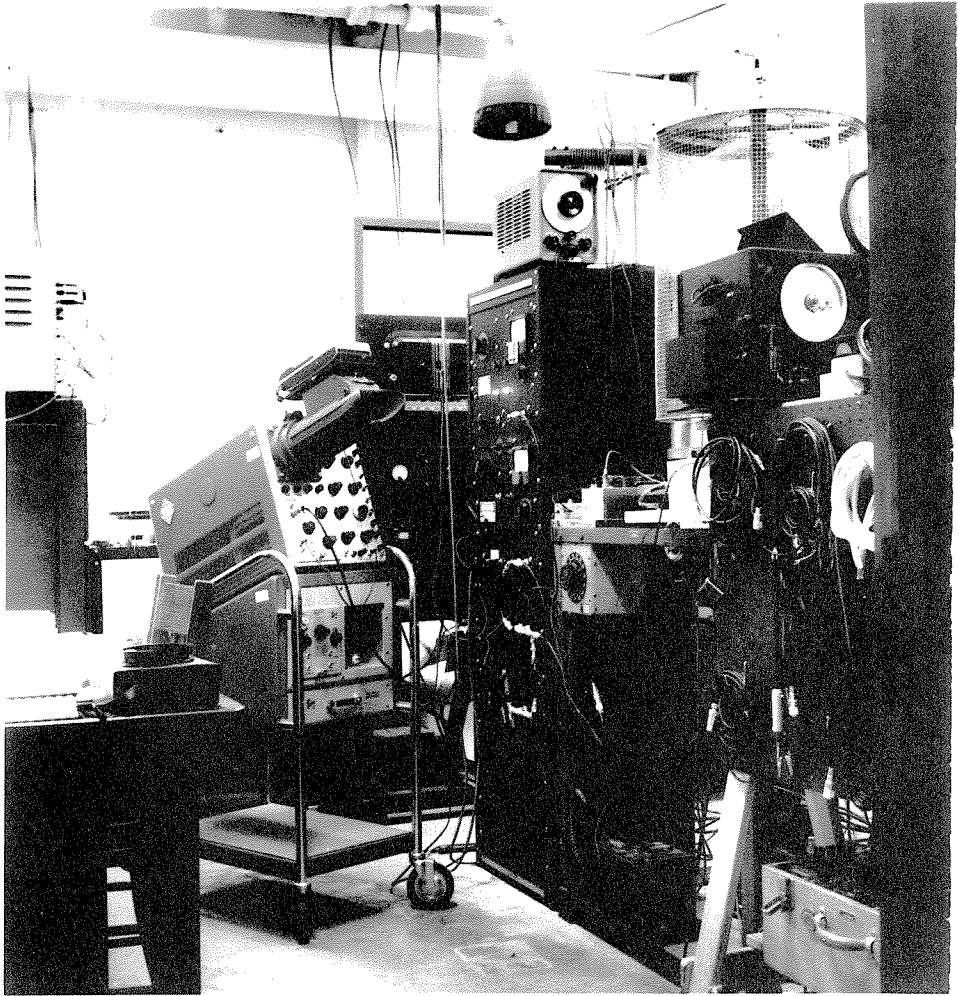


Fig. 2 - General view of the experimental assembly.

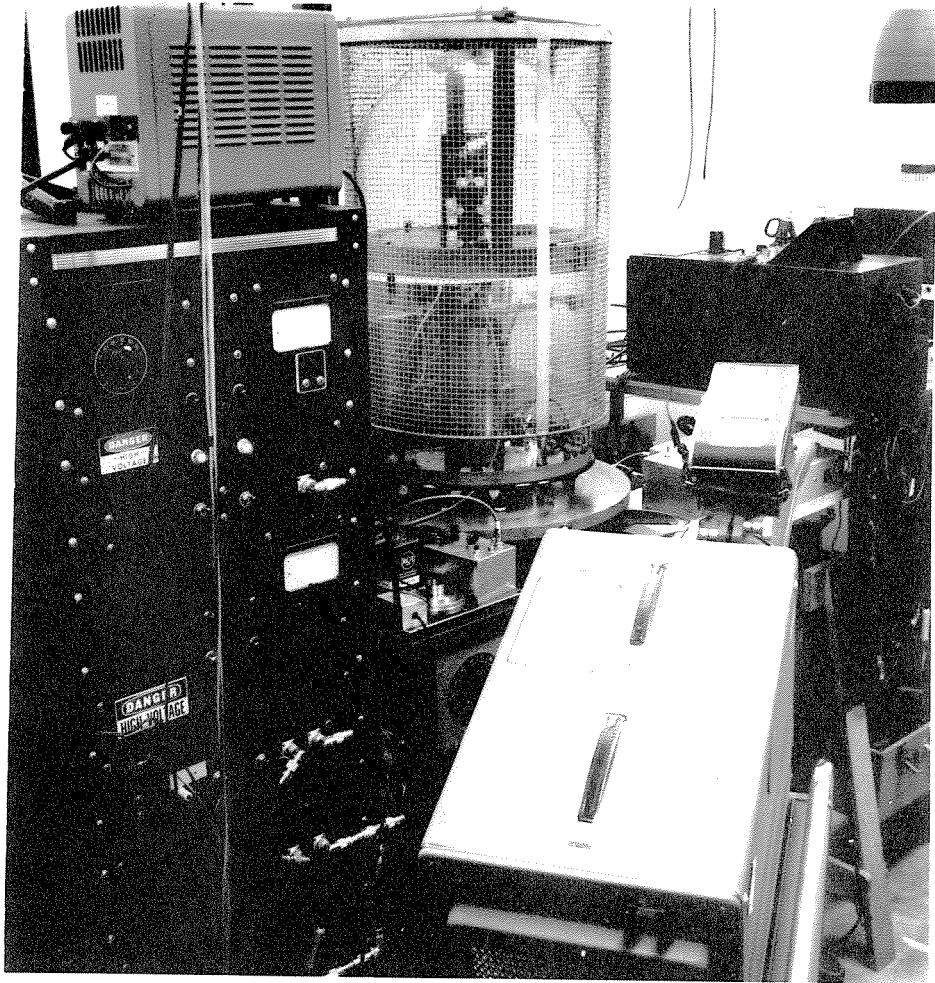


Fig. 3 - Portion of the experimental assembly showing (from left to right) the electronic control panel, the glass vacuum chamber with the furnace inside, and a Miller recording oscillograph. In the foreground is a Tektronix oscilloscope.

the specimen, the furnace, the temperature recording unit, and the electronic circuits used for heating the specimen will be described separately.

#### A. Specimen

The iron used in this investigation was procured from Johnson, Matthey and Co. Ltd. The original ingot, 5 mm in diameter, and 15 cm long, was drawn into a wire 0.020 inch in diameter. Variations in diameter were within  $\pm 2.5\%$ . This material contained the following interstitial impurities (in parts per million); carbon 300 ppm, oxygen 200 ppm, nitrogen 100 ppm. The metallic impurities, detected by spectrographic analysis, namely copper, nickel, silver, magnesium, and silicon amounted to less than 1 part per million of each.

After being drawn into a wire, the iron was subjected to a wet hydrogen treatment for decarburizing, followed by a dry hydrogen treatment for deoxygenizing <sup>(20)</sup>. The interstitial impurity content of the wire used in the experiment was:

Carbon	66 $\pm$	3 ppm
Oxygen	100 $\pm$	10 ppm
Nitrogen	192 $\pm$	2 ppm

The hydrogen treatment decreased both the carbon and oxygen contents, but, unfortunately, increased the nitrogen content.

Before the wire was spotwelded, three 60° V-notches were cut into the specimen, as shown in Fig. 4. The specimen was then cleaned

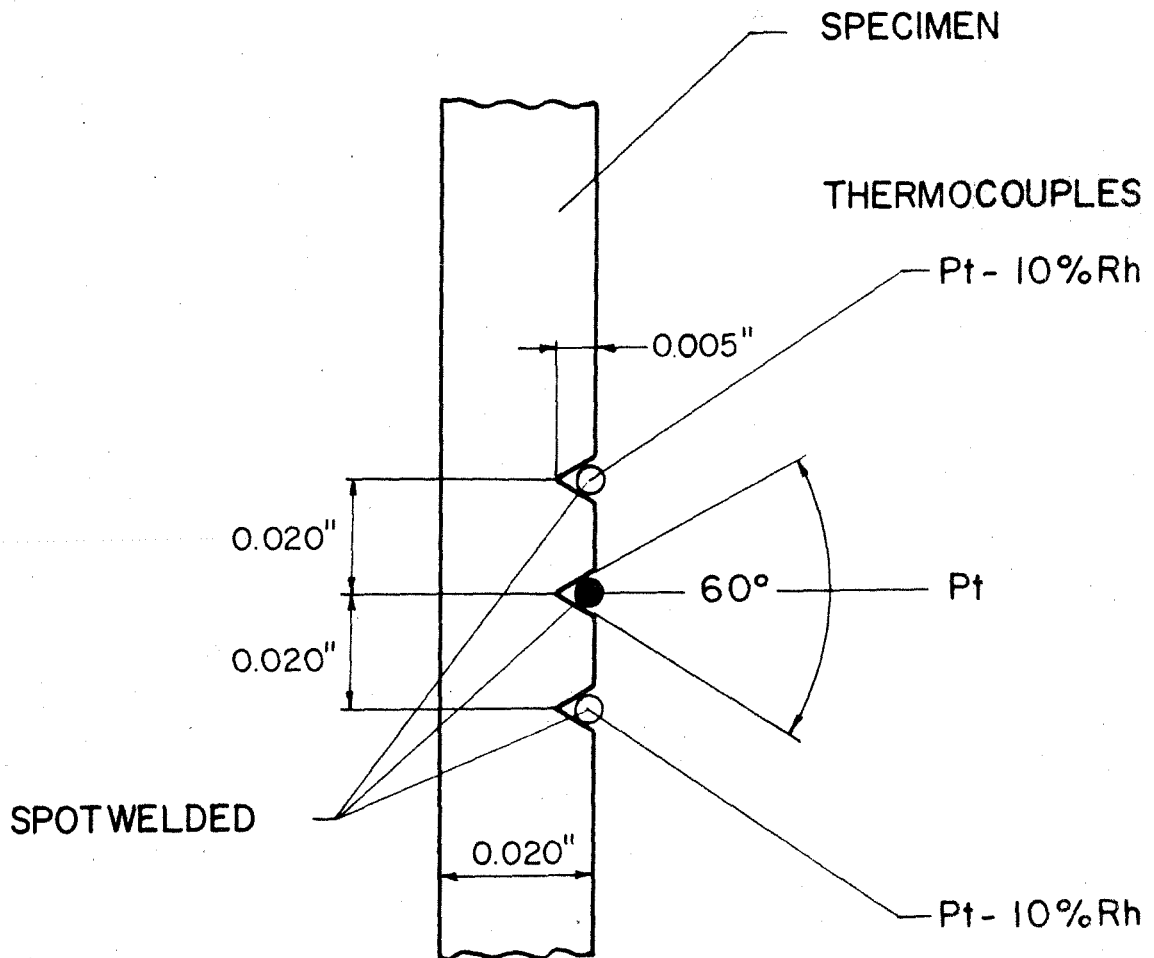


Fig. 4 - Sketch of the specimen with the attached thermocouple wires.

by immersion in trichlorethylene. In order to insure correct and reproducible positioning of the thermocouple wires, a special jig was built, as shown schematically in Fig. 5. The specimen A was fastened into the support assembly B, in the position it would occupy in the furnace. Two copper electrodes D were then pressed against the specimen (A) on one side and the thermocouple wire (C) on the other side. To avoid partial welding of the copper electrodes with either the specimen or the thermocouple wire, the tips of the electrodes were carefully cleaned with fine grain sand paper and methanol. A photograph of the spotwelding jig is also shown in Fig. 6.

#### B. Furnace

All experiments were performed in a furnace located in a vacuum chamber. This chamber, made of glass and shown in Fig. 2 and 3, respectively, was 24 inches in diameter and 36 inches tall. A vacuum of  $10^{-4}$  mm of mercury or better was obtained by using a 6 inch in diameter oil diffusion pump and a Kinney mechanical pump.

The requirements for the furnace were to achieve black body conditions and uniform temperature over the entire length of the specimen, namely 6 cm. To meet these requirements, the dimensions of the furnace chamber were chosen as 1-1/2 inches in diameter and 8 inches long. A schematic cross-section of the furnace is shown in Fig. 7, and a view of it is presented in Fig. 8. The heating element, made of kantal wire No. 19 (B&S), 0.036 inches in diameter, was wound uniformly around the cylindrical chamber made of ingot iron. The heating wire was

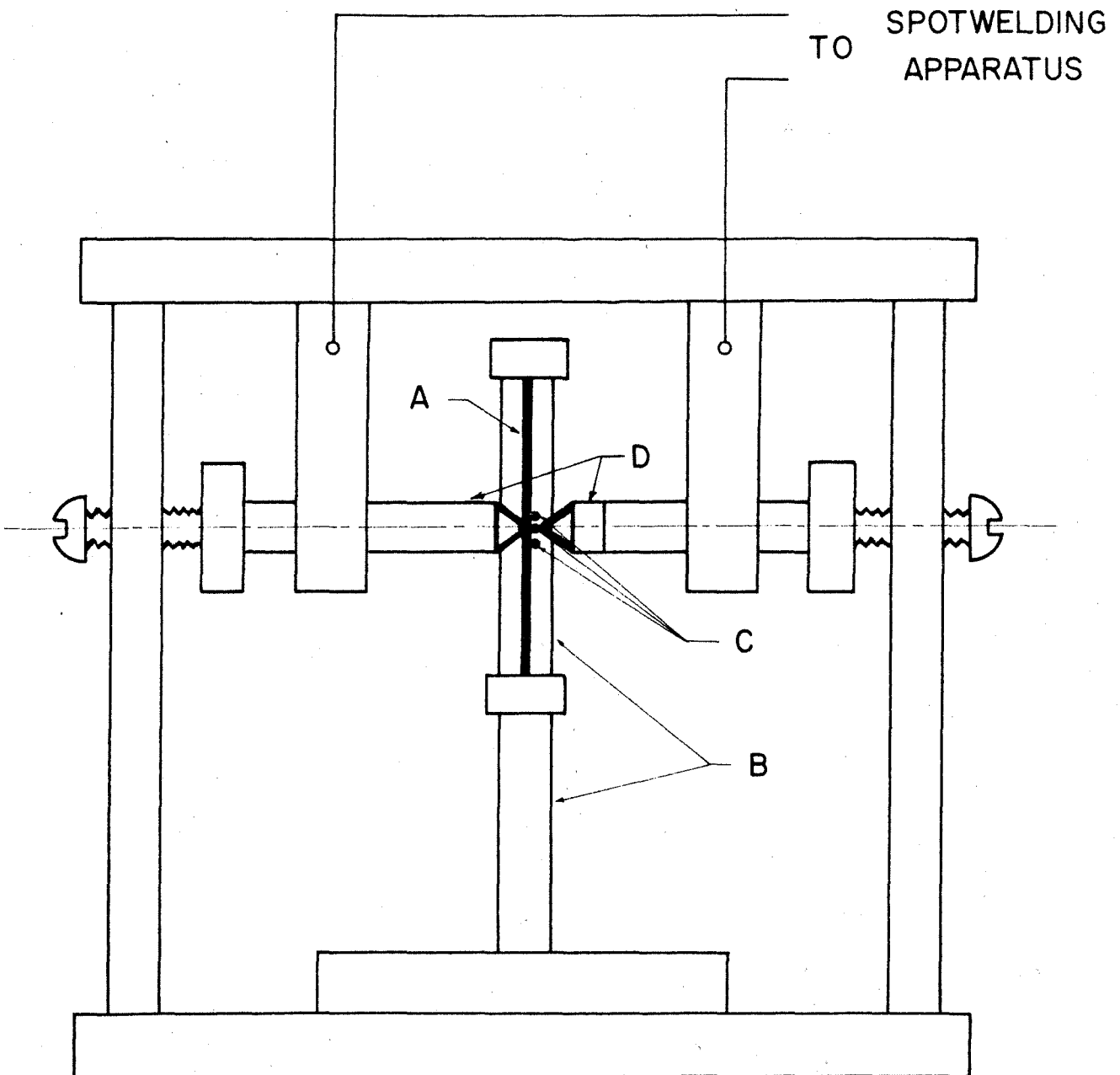


Fig 5 - Sketch of the spotwelding jig.

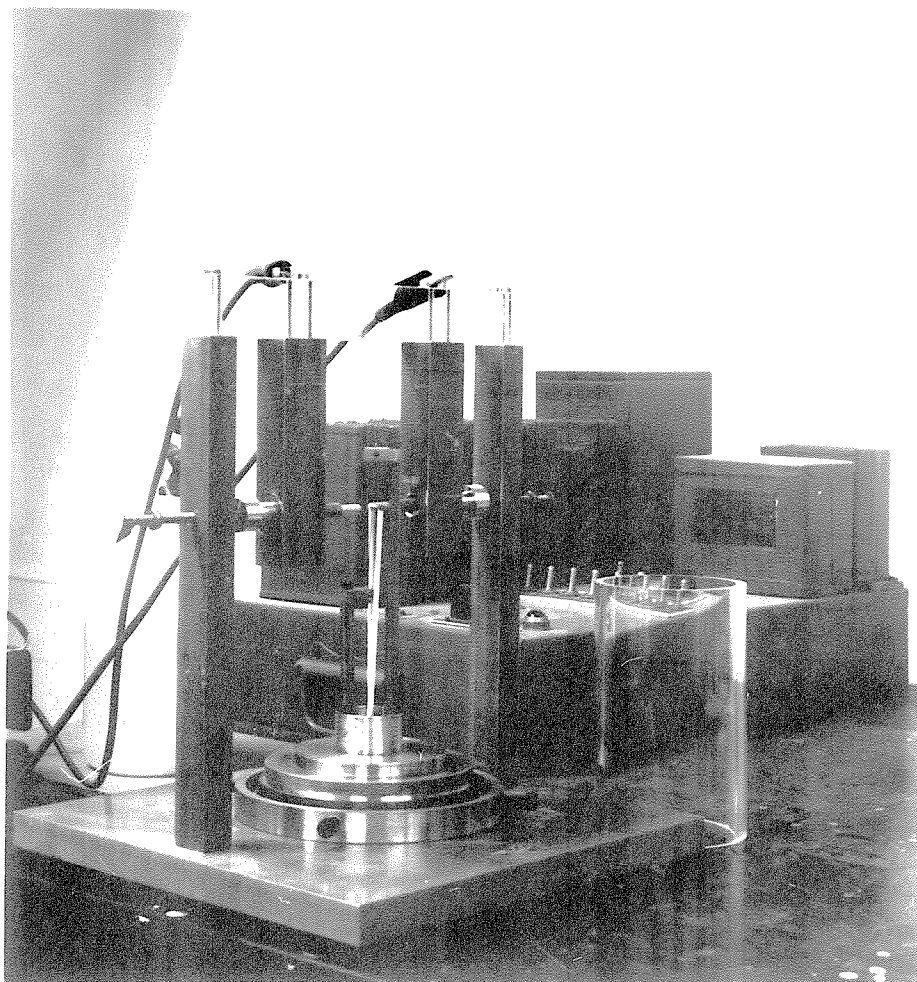


Fig. 6 - Spotwelding jig and spotwelding power supply.

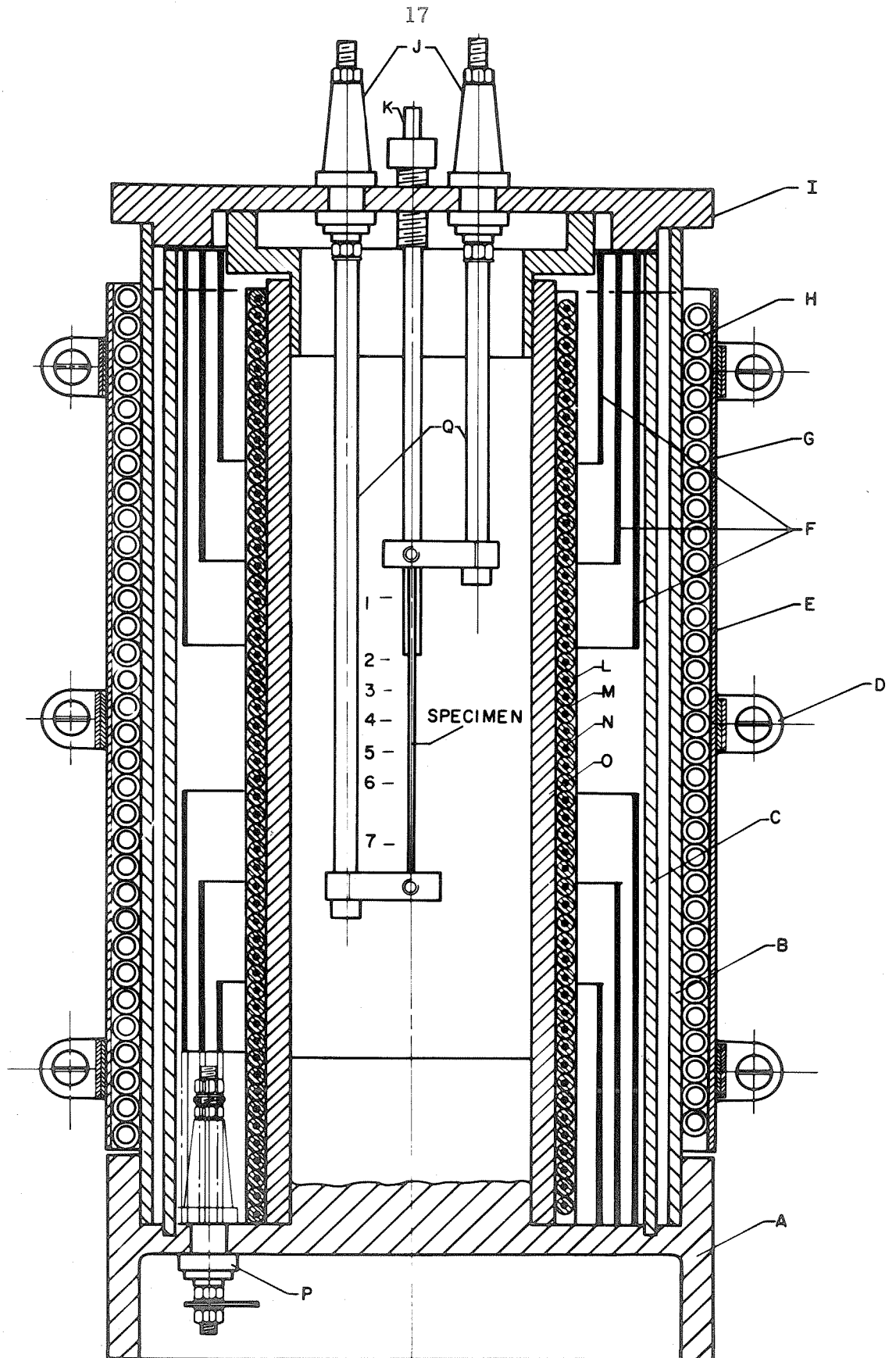


Fig. 7 - Schematic cross-section of the furnace.



KEY TO FIGURE 7

- A Base, (brass)
- B Outside Wall (brass)
- C Outside Heat Shield (low carbon steel)
- D Clamps (aluminum)
- E Jacket for Cooling Coil (sheet metal)
- F Heat Shields (low carbon sheet steel)
- G Jacket for Cooling Coil (sheet metal)
- H Cooling Coil (1/4" O.D. x 3/10" copper tube)
- I Cover (brass)
- J Connector to Specimen for Rate of Heating and Pulse Heating Experiments (Johnson No. 135-50)
- K Insulator, 2-hole, 6"lg, No. 22 wire
- L Jacket for Heating Coil (sheet of low carbon steel)
- M Alumina Fish Spin Beads No. 715-A
- N Heating Wire (Kantal 0.036 inch diameter)
- O Inside Wall (low carbon steel)
- P Connectors for Heating Coil (Johnson N 135-42)
- Q Support for Specimen
  
- 1,2,...7 Location of Thermocouples on Specimen for Temperature Tests of Furnace
  
- 4 Location of Thermocouples on Specimen for Rate of Heating and Pulse Heating Experiments

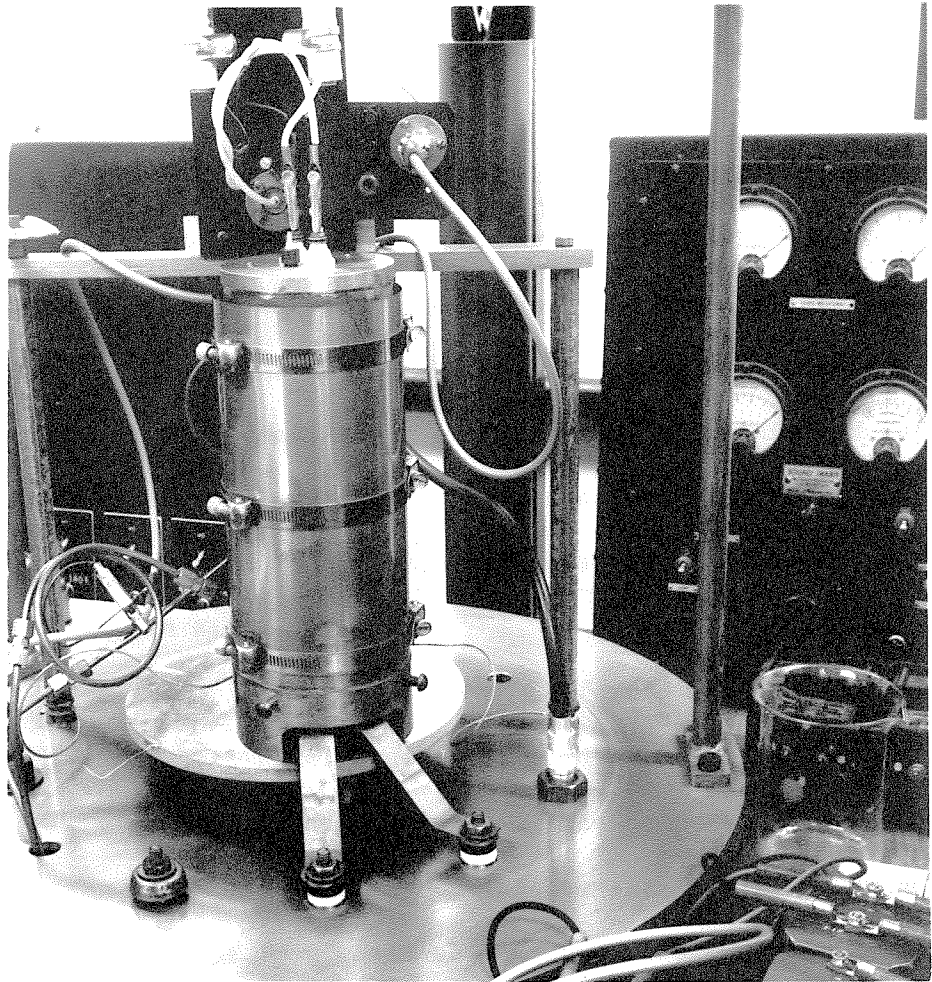


Fig. 8 - Front view of the furnace.

insulated by means of alumina "fish spine" beads. A brass cylinder was placed around the heating element and a water cooled copper coil was wrapped around the entire assembly. The maximum temperature obtained in the furnace was about 950 C, with an input power of about 800 watts.

Since the heat losses in a cylindrical uniformly wound furnace increase from the center to each extremity of the furnace, the temperature distribution along the axis of the furnace chamber was not uniform. To compensate for the variations in heat losses along the length of the furnace, a set of heat shields were introduced between the heating coil and the outside brass cylinder. The temperature along the axis of the furnace was measured at 7 different locations as shown in Fig. 7.

A series of experiments were performed and the optimum location for the heat shield was determined by trial and error. The beneficial effect of the heat shields on the temperature distribution in the furnace is shown in Fig. 9. The temperature distribution along the length of the specimen was also measured with the specimen electrically heated to a temperature above that of the furnace. The curves, shown in Fig. 10, were obtained with the furnace at 850 C, and the center of the specimen at 950 C, 1050 C, and 1150 C. Even under these conditions of non black body equilibrium, the temperature of the wire varied only within about  $\pm 3$  C over a distance of approximately  $\pm 1$  cm from the center of the wire.

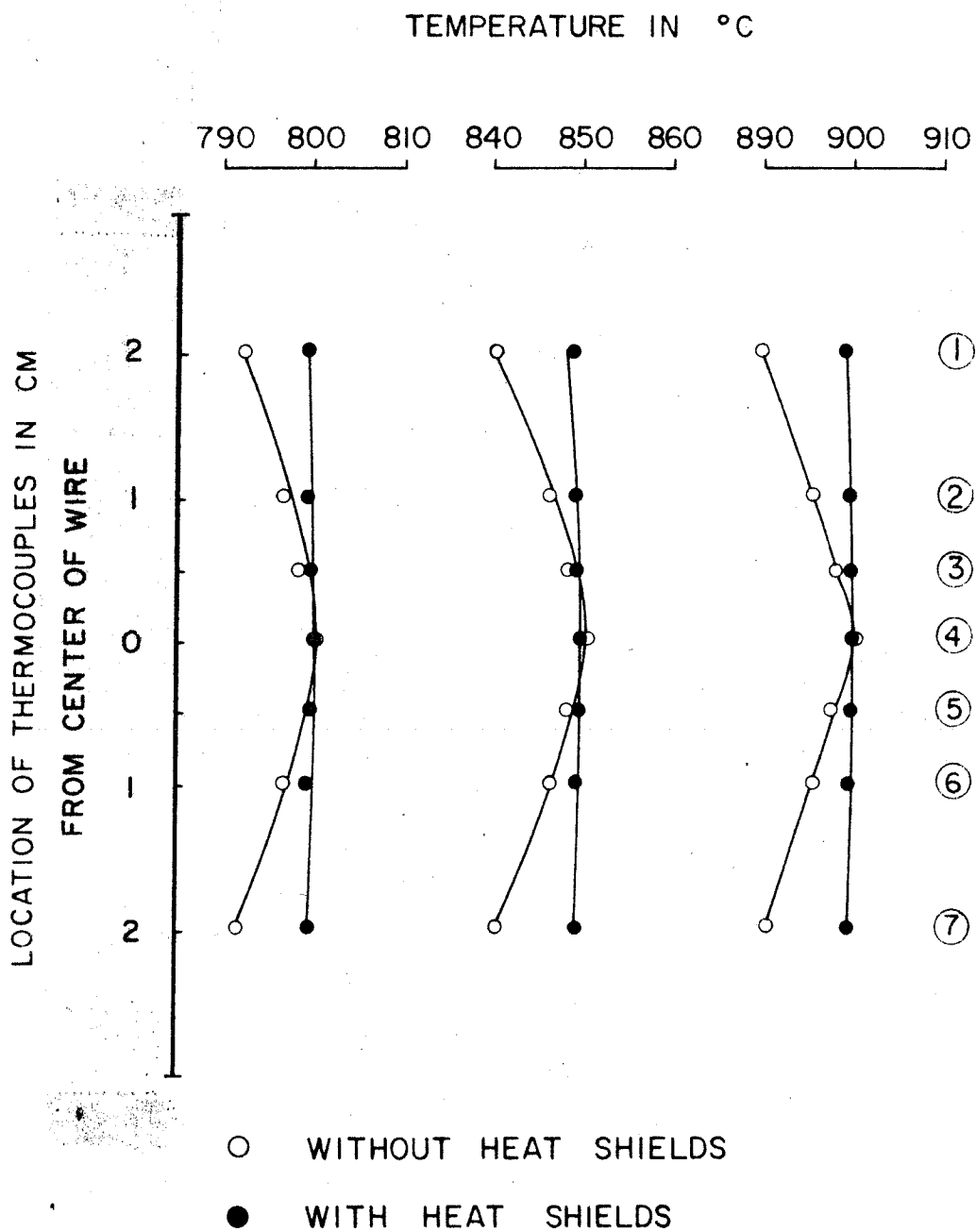
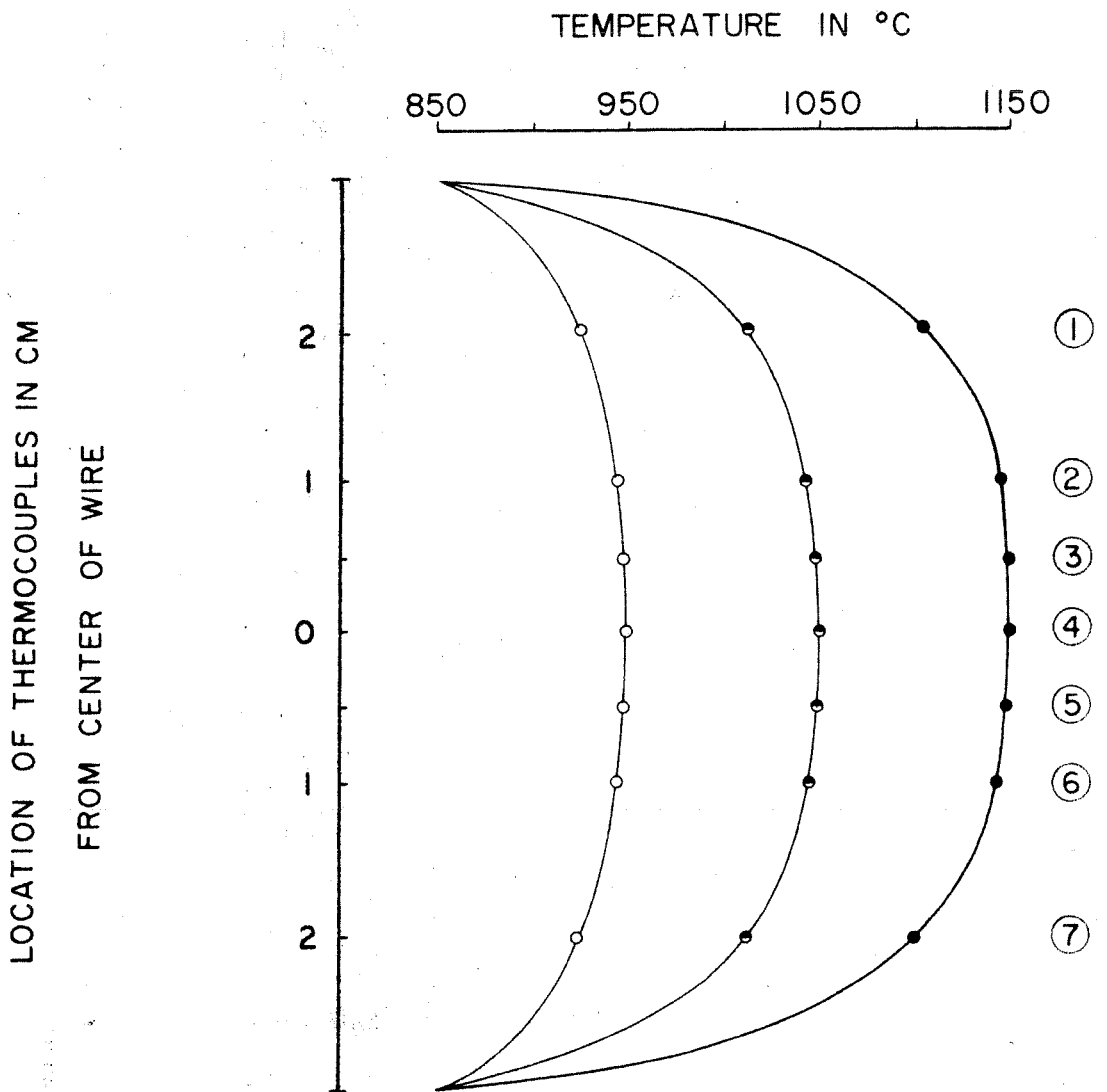


Fig. 9 - Temperature distribution along the specimen in the furnace under black body conditions.



- TEMPERATURE OF SPECIMEN AT ITS CENTER : 950 °C
  - ◐ TEMPERATURE OF SPECIMEN AT ITS CENTER : 1050 °C
  - TEMPERATURE OF SPECIMEN AT ITS CENTER : 1150 °C
- TEMPERATURE OF FURNACE : 850 °C

Fig. 10 - Temperature distribution along the specimen when the specimen is heated above the furnace temperature.

### C. Temperature Measurements

The first attempts to measure the temperature of the specimen were made by spotwelding two thermocouple wires, 0.005 inches in diameter, one made of platinum and the other of platinum-10% rhodium, at two points diametrically opposite on the specimen. This technique was unsatisfactory because an emf was generated in the thermocouple while a current was passing through the iron specimen, although the temperature of the specimen was not appreciably affected by the passage of current.

It was concluded that the thermocouple wires were not located exactly in an equipotential plane of the specimen and a fraction of current passing through the iron specimen was flowing into the thermocouple circuit. Attempts to improve the spotwelding technique were unsuccessful and an alternative scheme was developed. In this scheme, 3 thermocouple wires were spotwelded to the specimen at 3 points approximately 0.020 inches apart. The center wire was platinum, and the 2 outside wires were platinum-10% rhodium. The two latter ones were connected across the fixed resistance of a 10 ohm potentiometer. After passing a current through the specimen, the slider of the potentiometer was set so that no potential across A and B (see Fig. 11) was detectable any more. The complete wiring diagram of the thermocouple circuit is shown in Fig. 12. The thermal emf of the thermocouple was amplified by a DC amplifier with a gain of 30 decibels. The amplified signal was recorded on a rotating drum type oscillograph made by the

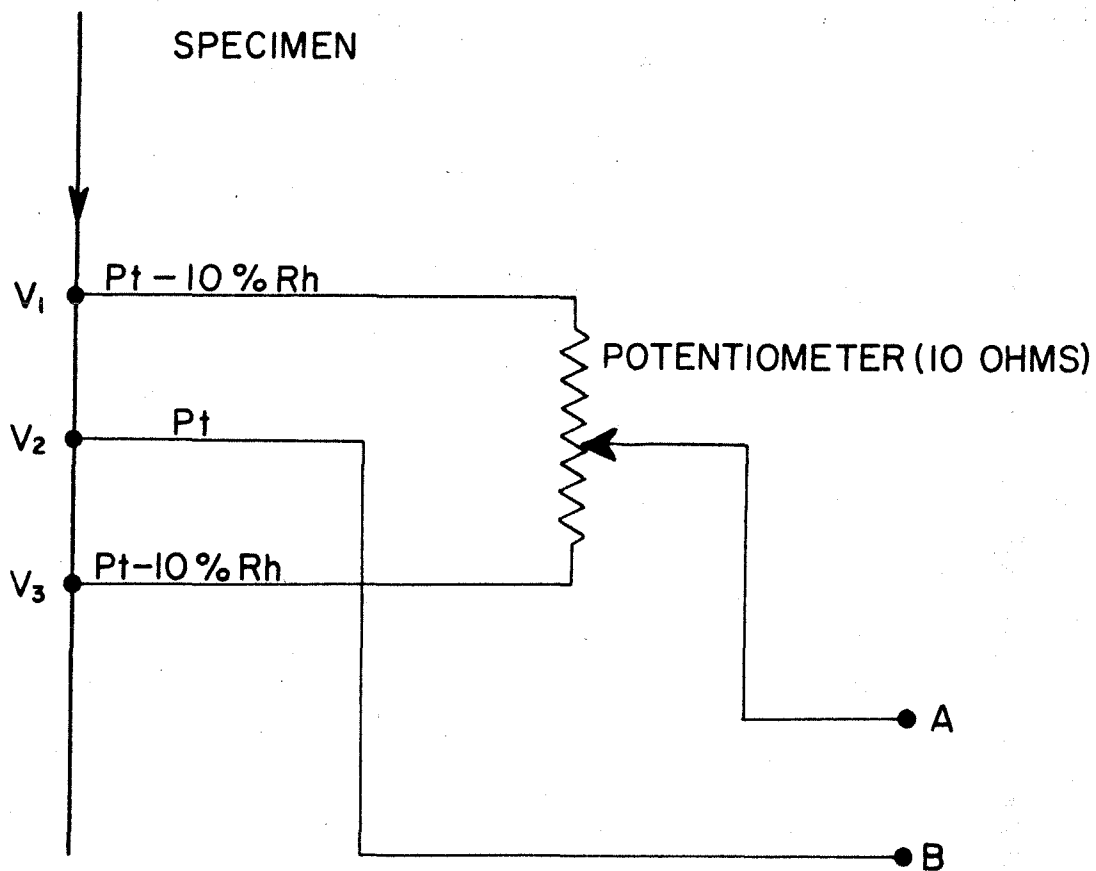


Fig. 11 - Diagram showing the method to nullify potentials due to non-thermal emf's along the specimen.

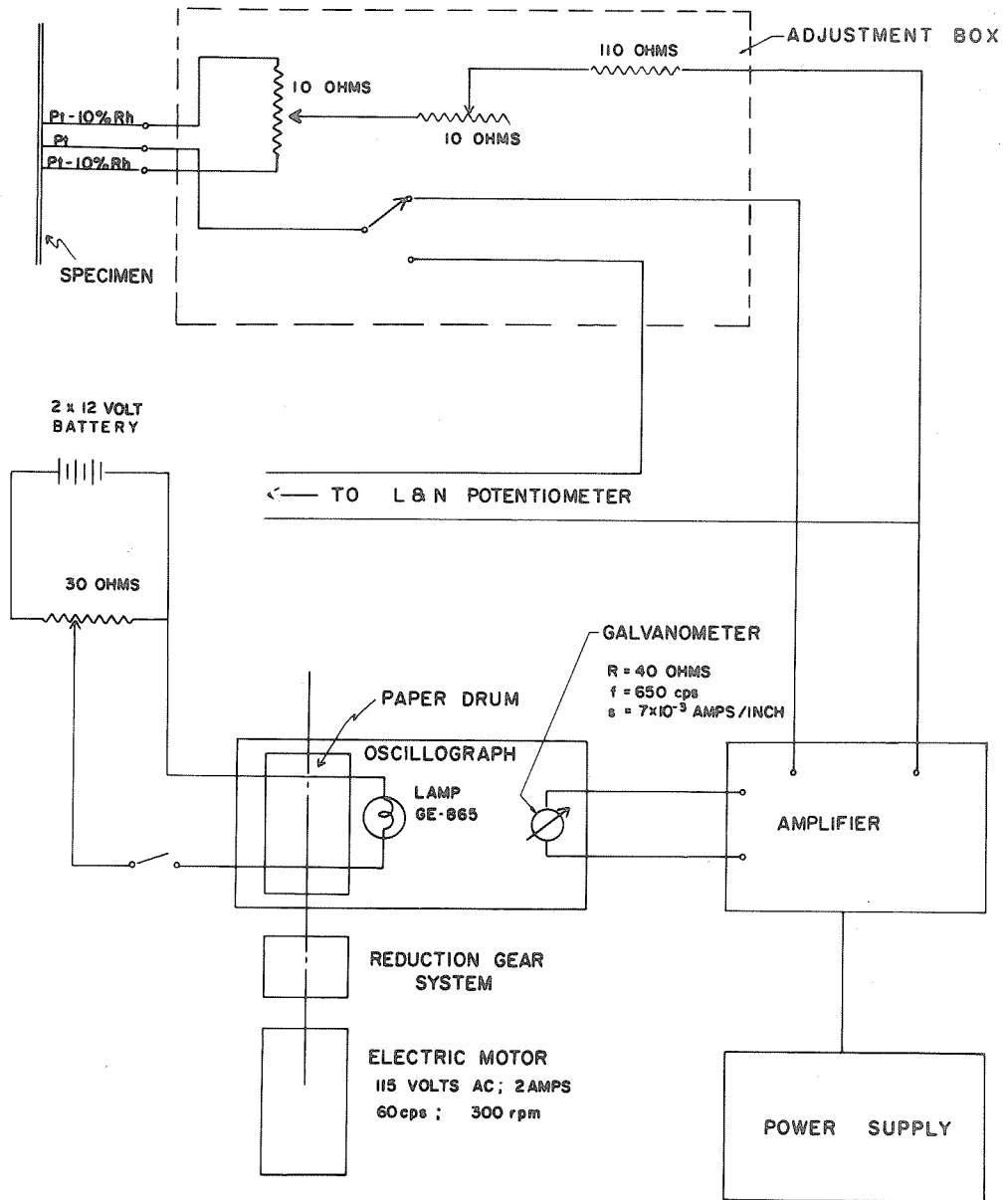


Fig. 12 - Wiring diagram of the recording unit.



William Miller Corporation in Pasadena, California. The galvanometer had a resistance of 40 ohms, and a nominal frequency of 650 cycles per second. The sensitivity was about 7 milliamperes per inch deflection. Four drum speeds were available, namely 5, 18, 35, and 75 cm per second. The temperature recording system was calibrated by measuring the galvanometer deflection corresponding to either a known emf input (indirect method) or an emf generated by a thermocouple placed in the furnace (direct method). The results obtained by both methods were in very good agreement, as shown in Fig. 13 (insert). A smooth curve traced through the experimental points was chosen as the final calibration curve and is shown in Fig. 13. It was possible to measure the galvanometer deflection within  $\pm 0.2$  mm and the temperature could be determined with an accuracy of  $\pm 0.5$  C. However, the presence of the experimental scatter in the calibration did not permit such a small tolerance and it was estimated that the temperature can be measured with an accuracy of  $\pm 5$  C only.

The wiring diagram for the calibration is shown in Fig. 14.

#### D. Rate of Heating Technique

One of the more common methods to achieve a constant heating rate in a specimen made out of conductive material is to apply a step function like voltage pulse across it. Different rates of heating can then be obtained by varying the pulse strength. A simple circuit, containing a switch, a variable resistor, and the specimen in series,

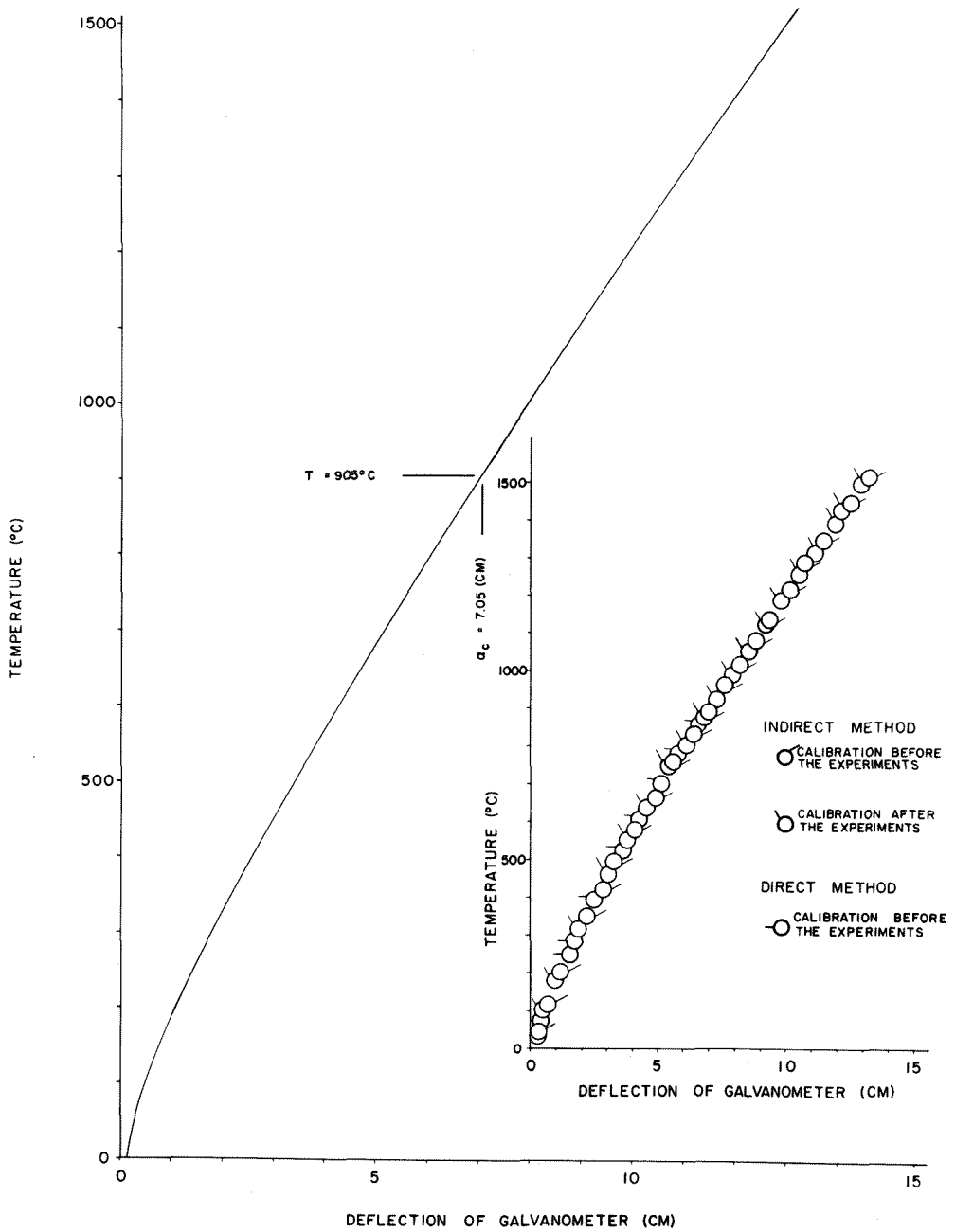


Fig. 13 - Calibration curve relating the galvanometer deflection to the temperature. The insert in the figure shows the actual measurements obtained by various methods.

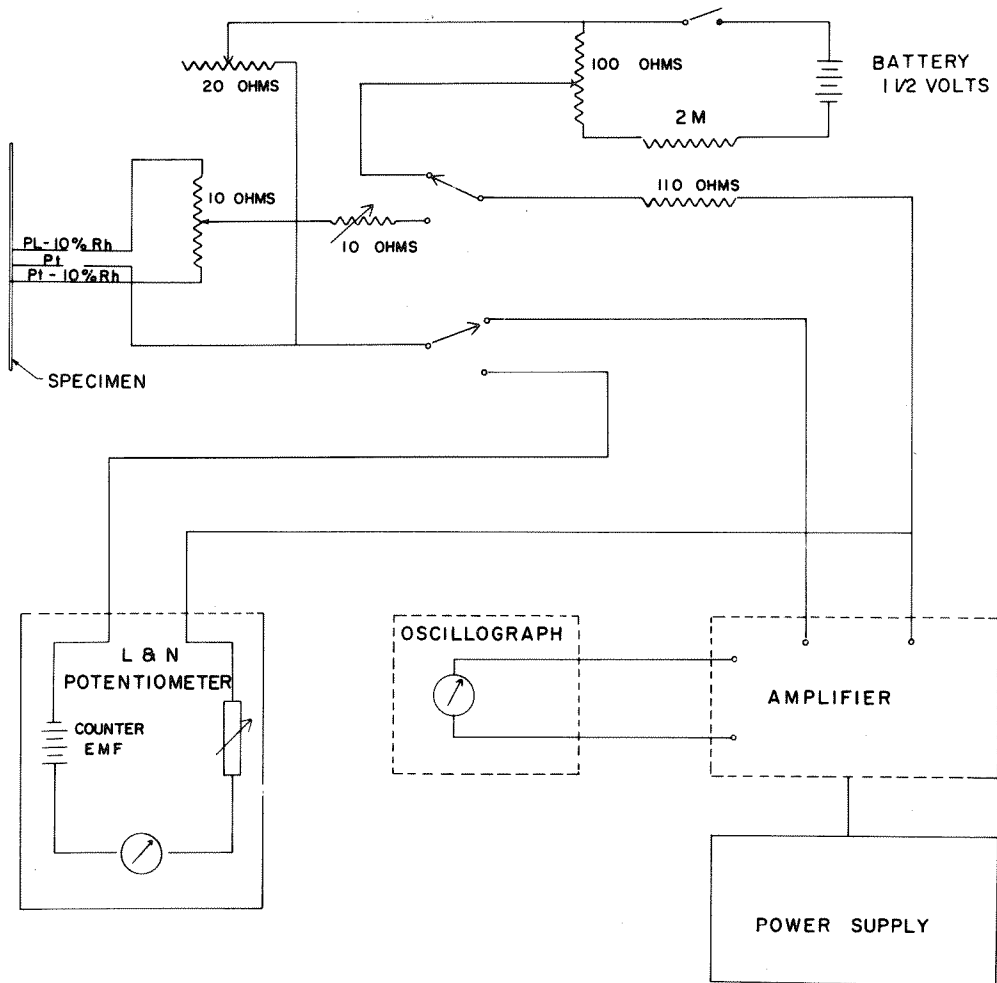


Fig. 14 - Wiring diagram for calibrating the recording galvanometer.

and connected to a suitable DC source (either a 24 volt high current battery or a DC line) can produce the desired voltage pulse across the specimen by merely closing the switch. Different pulse strength can then be obtained by varying the resistance of the circuit. This technique was used for the rate of heating experiments. This simple circuit, however, was included into a more complicated one, described in the next section of this chapter.

#### E. Pulse Heating Technique

The requirements set forth for the pulse-heating experiments were : 1) raise the temperature of the wire specimen from an initial value (between 800 and 900 C) to a higher temperature (as high as 1500 C) in the shortest possible time : 2) maintain this final temperature constant for as long as approximately 0.5 seconds. To achieve these conditions, it was necessary to heat the wire by means of two voltage pulses. The first pulse was a high voltage (1000 to 2000 v) pulse of short duration (about 700 microseconds). The second pulse was a relatively low voltage pulse (up to 20 v) and was sustained for several seconds. The circuit diagram with the details of the components is shown in Fig. 15. The short, high voltage pulse was generated in a transmission line consisting of seven segments of capacitors (28 microfarads) and inductors (0.1 millihenry). The impedance of this transmission line was about 2 ohms. The two pulses were initiated simultaneously by means of two thyratrons,  $TH_1$  and  $TH_2$  by

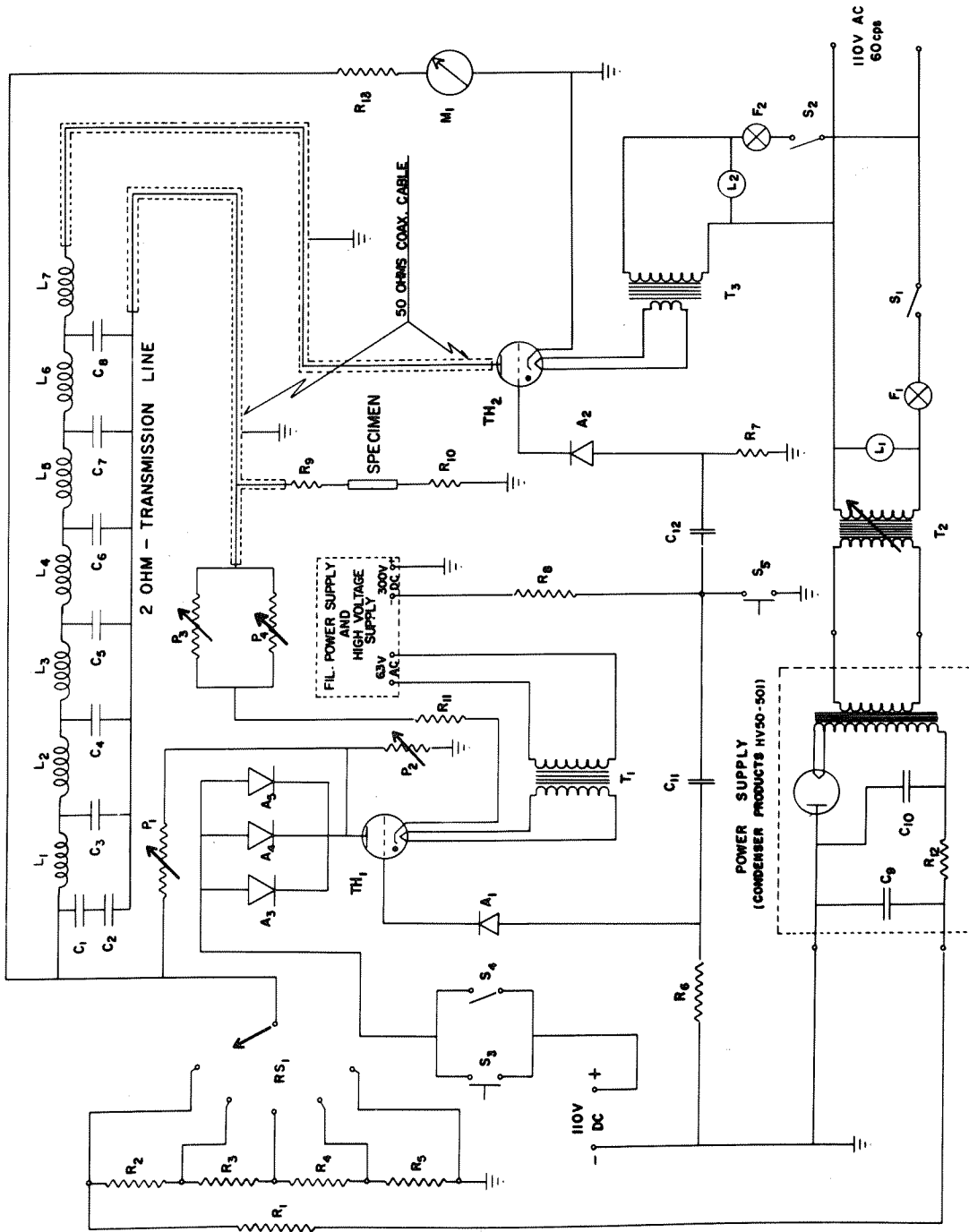


Fig. 15 - Circuit diagram of the pulse forming network.

KEY TO FIGURE 15

$A_1, A_2$	Germanium Diode (Sylvania Type IN 55A)
$A_3, A_4, A_5$	Silicon Rectifiers (Sarkes Tarzian Inc., Rectifier Division, Type S-5018)
$C_1, C_2, \dots, C_8$	Capacitors (2.8 microfarad)
$C_9, C_{10},$	Capacitors (0.1 microfarad)
$C_{11}, C_{12},$	Capacitors (.001 microfarad)
$F_1, F_2,$	Fuses (110 V, 3 amp.)
$L_1, L_2, \dots, L_6,$	Inductors (0.1 millihenry)
$L_7,$	Inductor (0.05 millihenry)
M	DC Voltmeter 0-2500 V (Simpson Model 29)
$P_1, P_2,$	Potentiometer (0-1 Meg.)
$P_3,$	Potentiometer (0-50 ohm)
$P_4,$	Potentiometer (0-10 ohm)
$R_1,$	Resistor (1 Meg.)
$R_2,$	Resistor (0.45 Meg.)
$R_3,$	Resistor (0.5 Meg.)
$R_4,$	Resistor (0.6 Meg.)
$R_5,$	Resistor (0.8 Meg.)
$R_6, R_7, R_8,$	Resistor 10 K

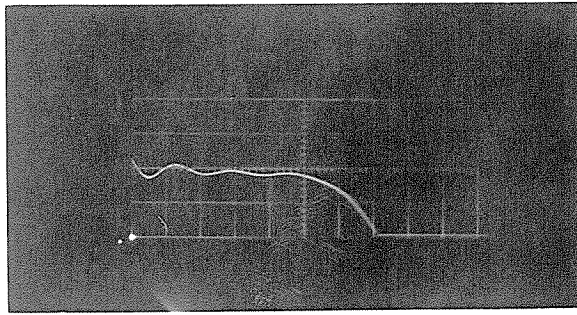
R <sub>9</sub> , R <sub>10</sub> ,	Resistor 1 ohm
R <sub>11</sub> ,	Resistor 10 ohm
R <sub>12</sub> ,	Resistor 2 Meg.
R <sub>13</sub> ,	Resistor 50 K
RS	Rotary Switch (Mallory, 1 set, 2 to 6 pos. & off.)
S <sub>1</sub> , S <sub>2</sub> ,	Toggle Switch (3 amp.)
S <sub>3</sub> ,	Push Button Switch (10 amp.)
S <sub>4</sub> ,	Toggle Switch (10 amp.)
S <sub>5</sub> ,	Push Button Switch
T <sub>1</sub> ,	Isolation Transformer (TRIAD Type N-54M)
T <sub>2</sub> ,	Powerstat (Superior Electric Co. Type 20)
T <sub>3</sub> ,	Filament Transformer (TRIAD Type F-21A)
TH <sub>1</sub> ,	Hydrogen Thyatron (Kulhe Laboratories 4C 35)
TH <sub>2</sub> ,	Hydrogen Thyatron (Phillips Laboratories 5C22)

closing switch  $S_5$ . It was necessary, however, to boost up the voltage of the anode of the thyatron ( $TH_1$ ) connected with the energy source for the low voltage long duration pulse by applying an "artificial" high voltage to this tube prior to firing. The high voltage power supply used for charging the transmission line was used for this purpose. However, in order to isolate the energy source of the low voltage long duration pulse, a set of 3 silicon rectifiers (in parallel) were inserted between the anode of the thyatron and the positive side of the 110 Volts DC source. The different levels of strength for the short duration high voltage pulse were obtained through the proper setting of a Variac Transformer in the low voltage side of the power supply. An additional means of changing the pulse strength was provided by inserting a certain number of resistors in series in the high voltage line. These resistors were then properly connected to a 6 position rotary switch  $RS_1$  (see Fig. 15).

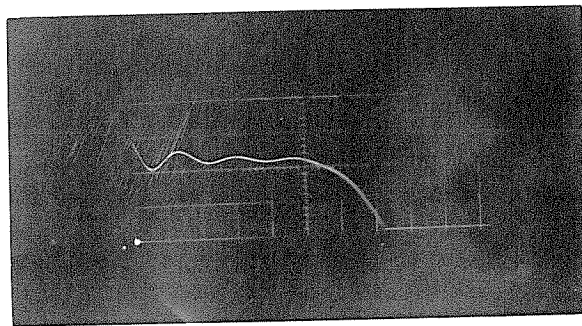
The applied voltage pulse - the shape of three typical ones is shown in Fig. 16 - have a short rise time which may cause an appreciable skin effect in the specimen. This effect has been analyzed in the Appendix of this thesis and the result shows that the skin depth is large compared with the diameter of the wire. Thus, the heating of the wire may be considered as uniform for all practical purposes. The basic information needed for the design of the pulse forming network was found in Glasoe & Lebacqz, <sup>(21)</sup> LePage & Seely, <sup>(22)</sup> Millman & Taub, <sup>(23)</sup> and Thomason <sup>(24)</sup>.

---

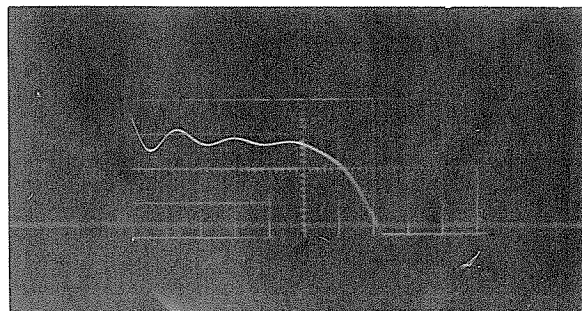




V = 800 volts



V = 1100 volts



V = 1400 volts

Fig. 16 - Three voltage pulses showing different strength. The grid spacing corresponds to 100 microseconds.

#### IV EXPERIMENTAL RESULTS

##### A. Rate of Heating Experiments

In these experiments, a single voltage pulse was applied and the temperature of the specimen increased at a certain rate, depending on the strength of the pulse. The temperature at which the latent heat of transformation was released was located on the temperature - time record by a rather sudden change in slope. A typical record is shown in Fig. 17. In this record, it is apparent that the rate of heating between the initial temperature and the temperature at which the latent heat was released was not exactly constant, but decreased slightly with increasing temperature. The data were analyzed on the basis of an average rate of heating defined as the average slope of the temperature vs. time curve in the range of temperatures between the equilibrium transformation temperature and the temperature at which the latent heat was released. A graphical illustration of the determination of this average slope is shown in Fig. 18.

If absolutely pure iron had been used for these experiments, any temperature just below that of the alpha to gamma transformation temperature (905 C) could have been used as the initial temperature  $T_1$ . Because of the presence of interstitial impurities in the iron, a two phase region, alpha plus gamma exists in the quaternary diagram iron-oxygen-nitrogen-carbon. As shown in Fig. 19, oxygen has practically no effect on the alpha to gamma transformation, and the presence of

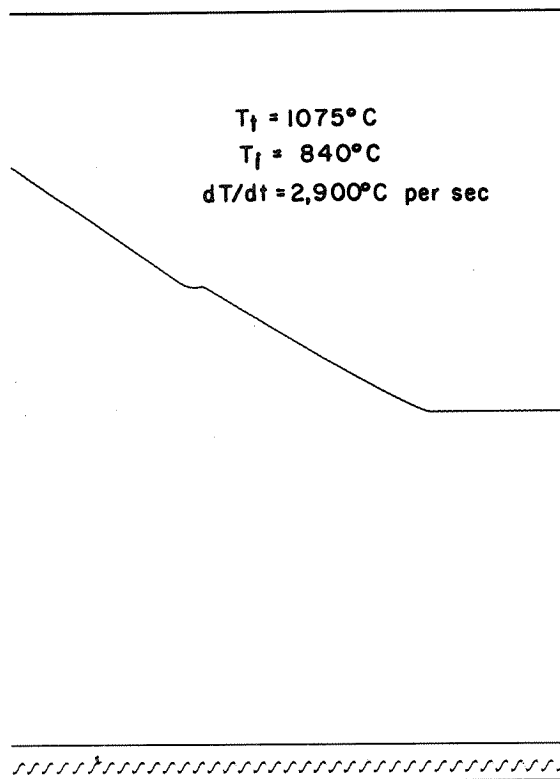


Fig. 17 - Typical record of the temperature of the specimen versus time in a rate of heating experiment. The time scale increases from right to left and was determined from the 500 cycle per second oscillograph trace shown at the bottom of the record.

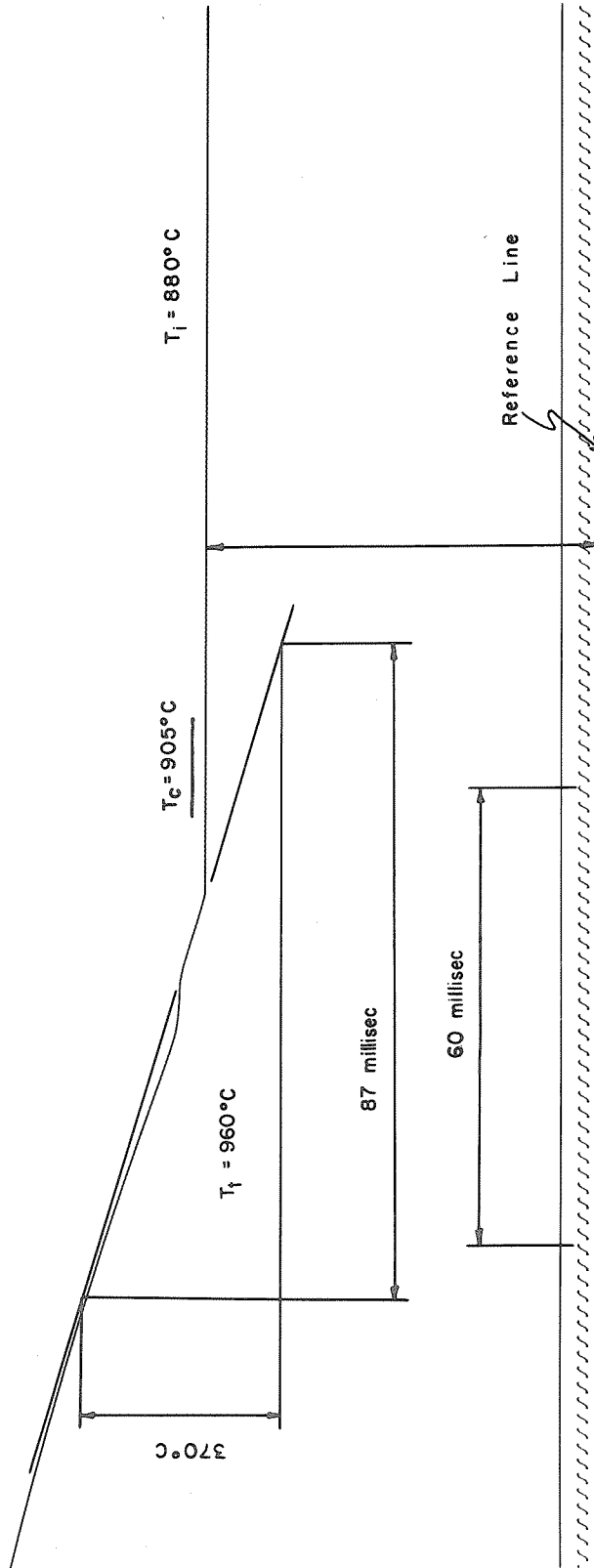
$$dT/dt = 4250^{\circ}\text{C per sec}$$


Fig. 18 - Typical record of a rate of heating experiment showing the graphical technique used for determining the rate of heating.

this impurity can be neglected. The exact phase boundaries of the alpha plus gamma field in ternary alloys iron-carbon-nitrogen could not be found in the literature, but the binary systems iron-carbon and iron-nitrogen have been extensively studied. Portions of the phase diagrams of these two binary systems were produced in Fig. 20 and 21, respectively. The impurity content of the material used in this investigation is indicated by a vertical line in both figures. Since carbon and nitrogen concentrations are relatively small, it may be assumed that, in the ternary diagram iron-carbon-nitrogen, the surface separating the alpha from the alpha plus gamma fields is very close to a plane passing through the two corresponding boundaries in the binary systems. Following this assumption, it is possible to determine the phase boundary temperature in the ternary system. This temperature is approximately 870 C. A somewhat lower temperature, namely 840 C, was chosen as initial temperature for the first series of rate of heating experiments.

About 40 experiments were performed with various rates of heating ranging from about 100 to 7000 C per second. Five typical temperature versus time records are shown in Fig. 22. In all records, the break in the curve due to the release of the latent heat of transformation was quite sharp, and could be located on the original record within  $\pm 0.5$  mm. The resulting uncertainty in the temperature measurement was  $\pm 5$  C. The rate of heating, measured as explained at the beginning of this chapter, was obtained with an

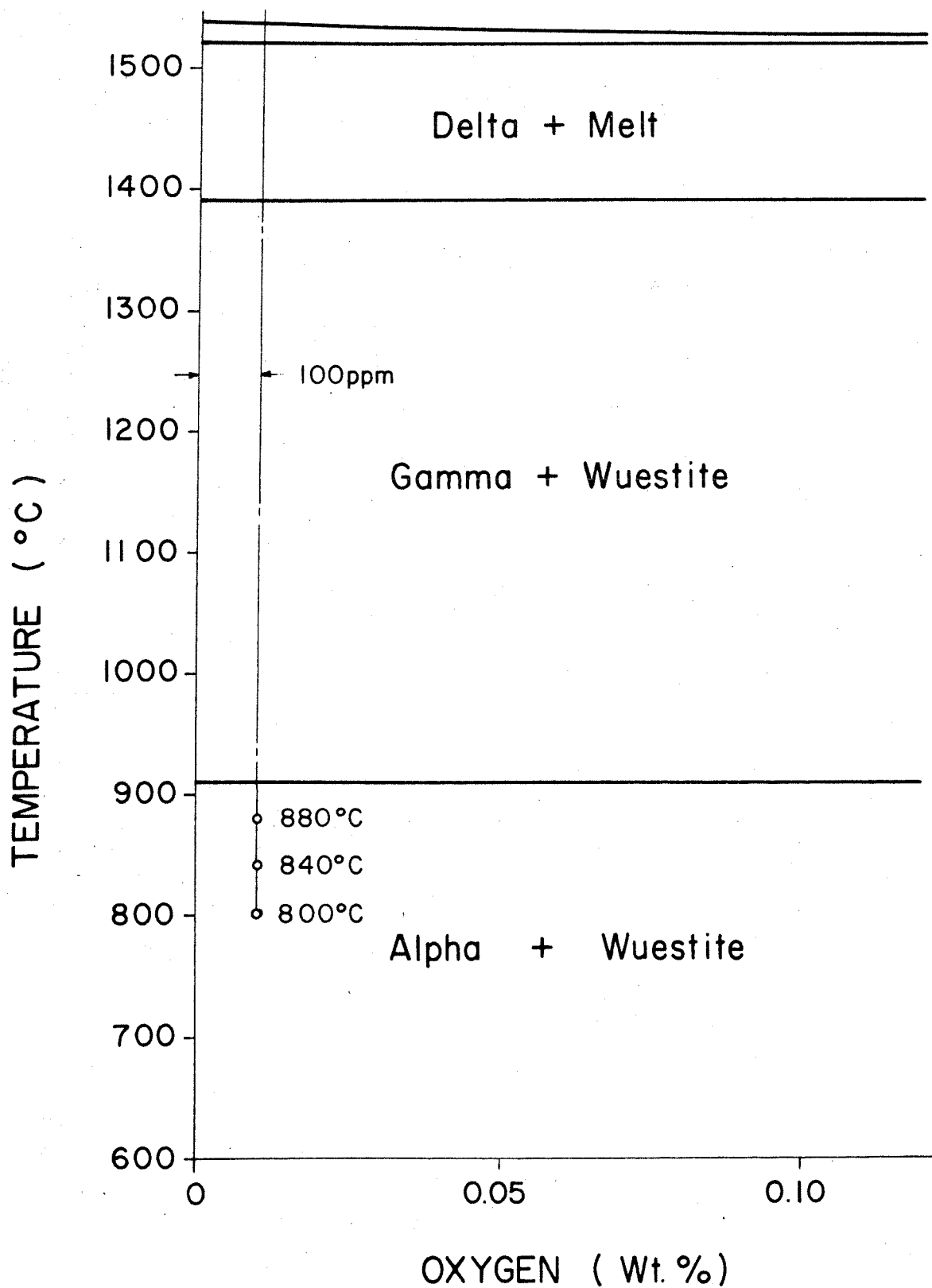


Fig. 19 - Partial phase diagram of the iron-oxygen system (from Hansen, M.: "Constitution of Binary Alloys," McGraw-Hill, 1958).

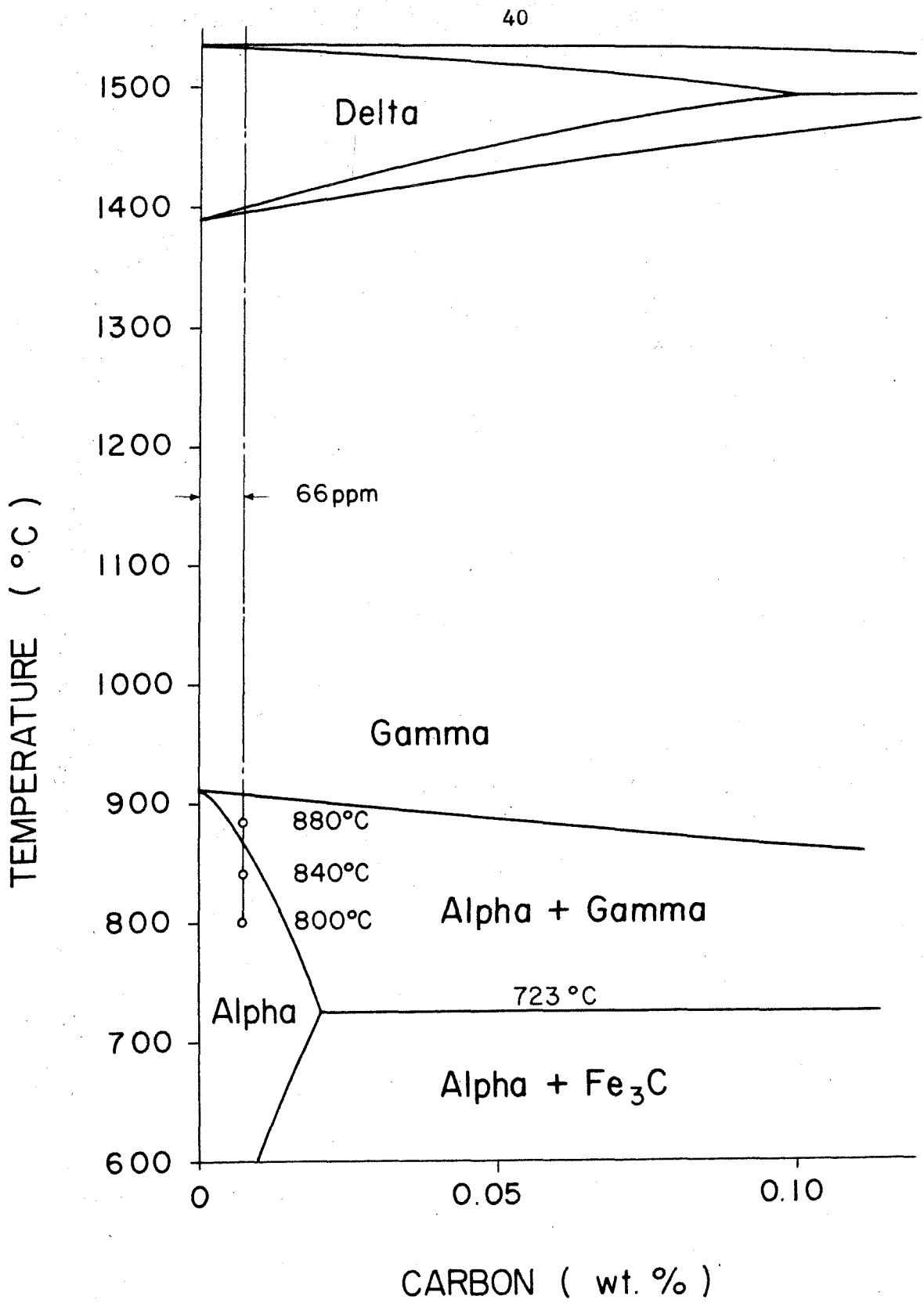


Fig. 20 - Partial phase diagram of the iron-carbon system (from Hansen, M.: "Constitution of Binary Alloys," McGraw-Hill, 1958).

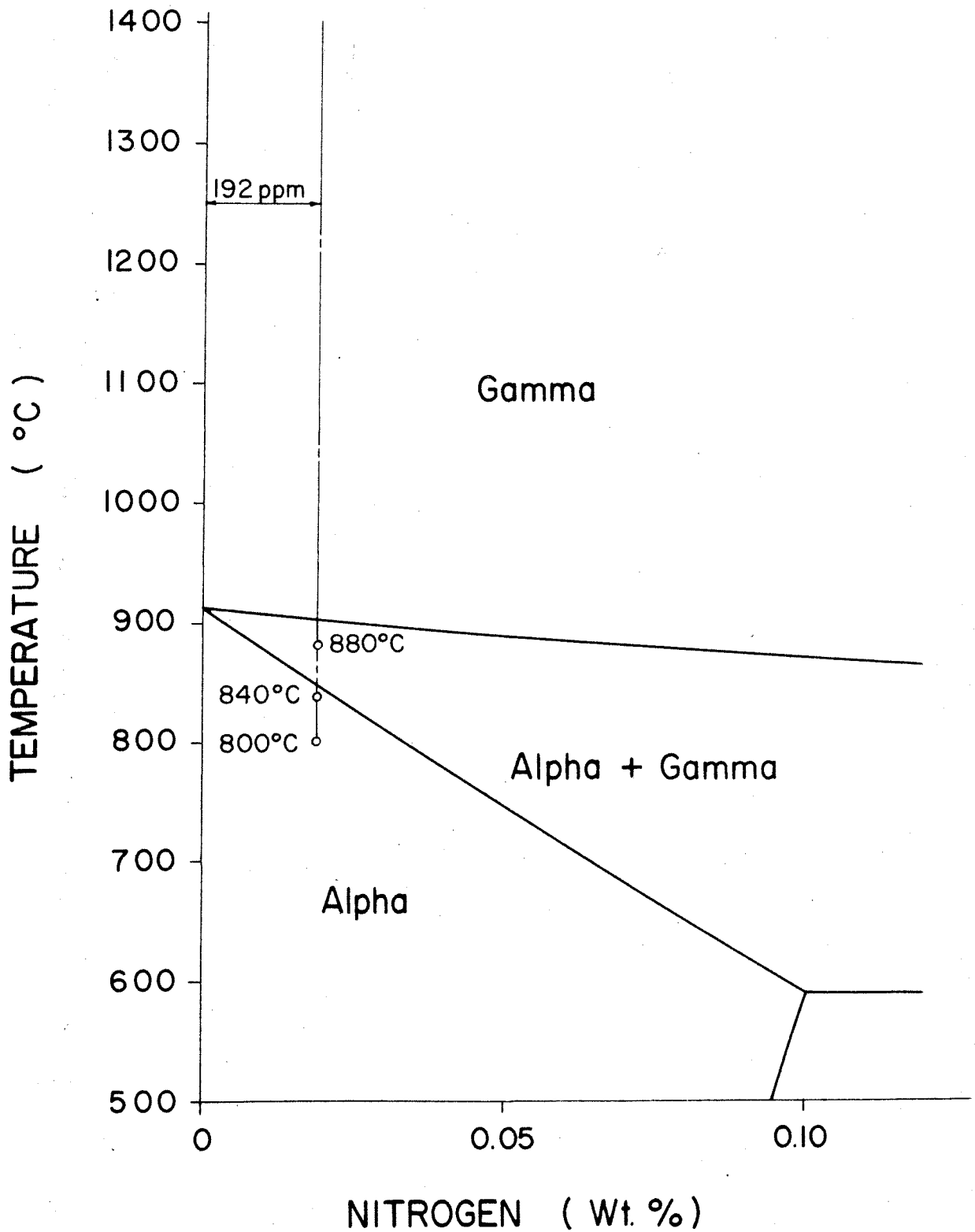


Fig. 21 - Partial phase diagram of the iron-nitrogen system (from Hansen, M.: "Constitution of Binary Alloys," McGraw-Hill, 1958).



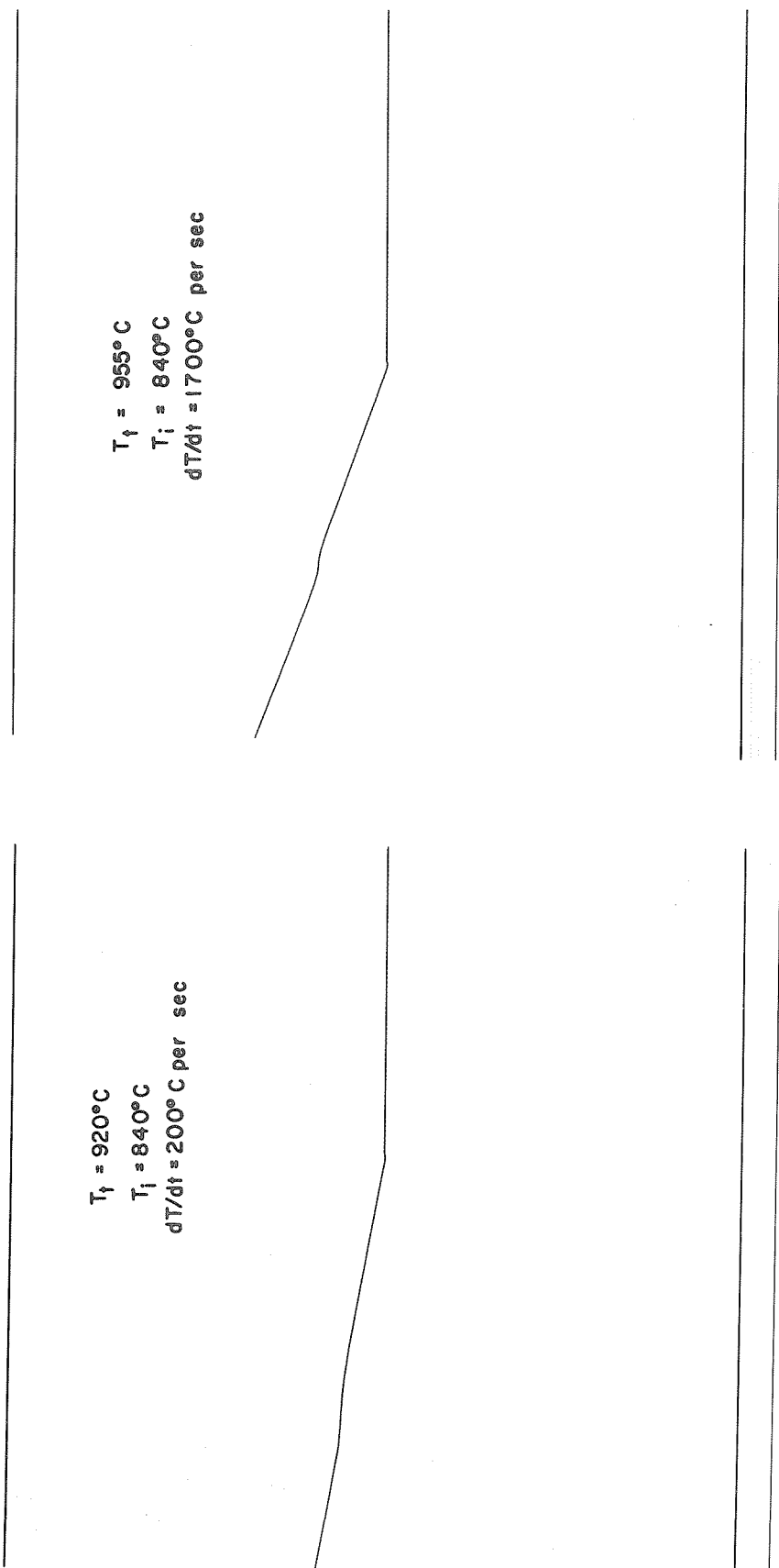


Fig. 22 - Typical records from rate of heating experiments.  
Initial Temperature  $T_i = 840\text{ C}$ .

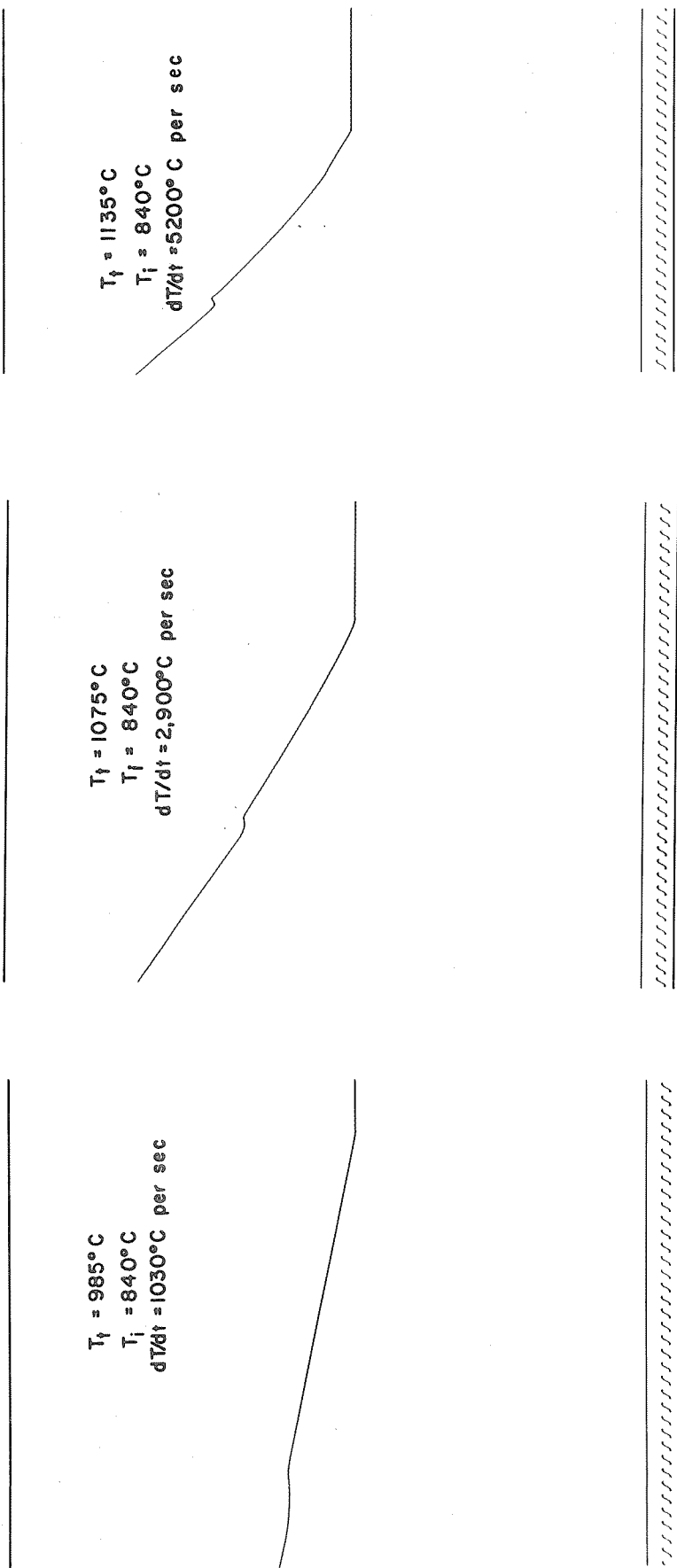


Fig. 22 - Typical records from rate of heating experiments.  
(cont.) Initial temperature  $T_i = 840^\circ\text{C}$ .

uncertainty of  $\pm 15\%$ .

The results of all measurements are shown in Fig. 23. The uncertainty in the temperature corresponds to the size of the circles, and a horizontal segment of line represents the uncertainty in the rate of heating. As it was anticipated, the rate of heating raises the allotropic transformation of iron. The effect of rate of heating is more pronounced than that of rate of cooling. At a rate of 5000 C per second, for example, the alpha to gamma transformation is depressed about 140 C by cooling <sup>(15)</sup> and is raised about 220 C by heating. Another important fact to point out is that above a rate of heating of about 8000 C per second, no thermal arrest on the temperature versus time records could be detected. This result will be discussed in section C of this chapter.

The effect of the presence of some gamma phase in the specimen before the heating pulse was applied was determined in a second series of experiments performed with an initial temperature of 880 C. Five typical records from these experiments are presented at Fig. 24. As shown in Fig. 20 and 21, 880 C is above the alpha to gamma boundaries in both iron-carbon and iron-nitrogen phase diagrams. The results of these experiments are shown in Fig. 23 (black circles).

#### B. Pulse Heating Experiments

In these experiments the temperature of the specimen was increased from its initial value to its final value in about 700 micro-

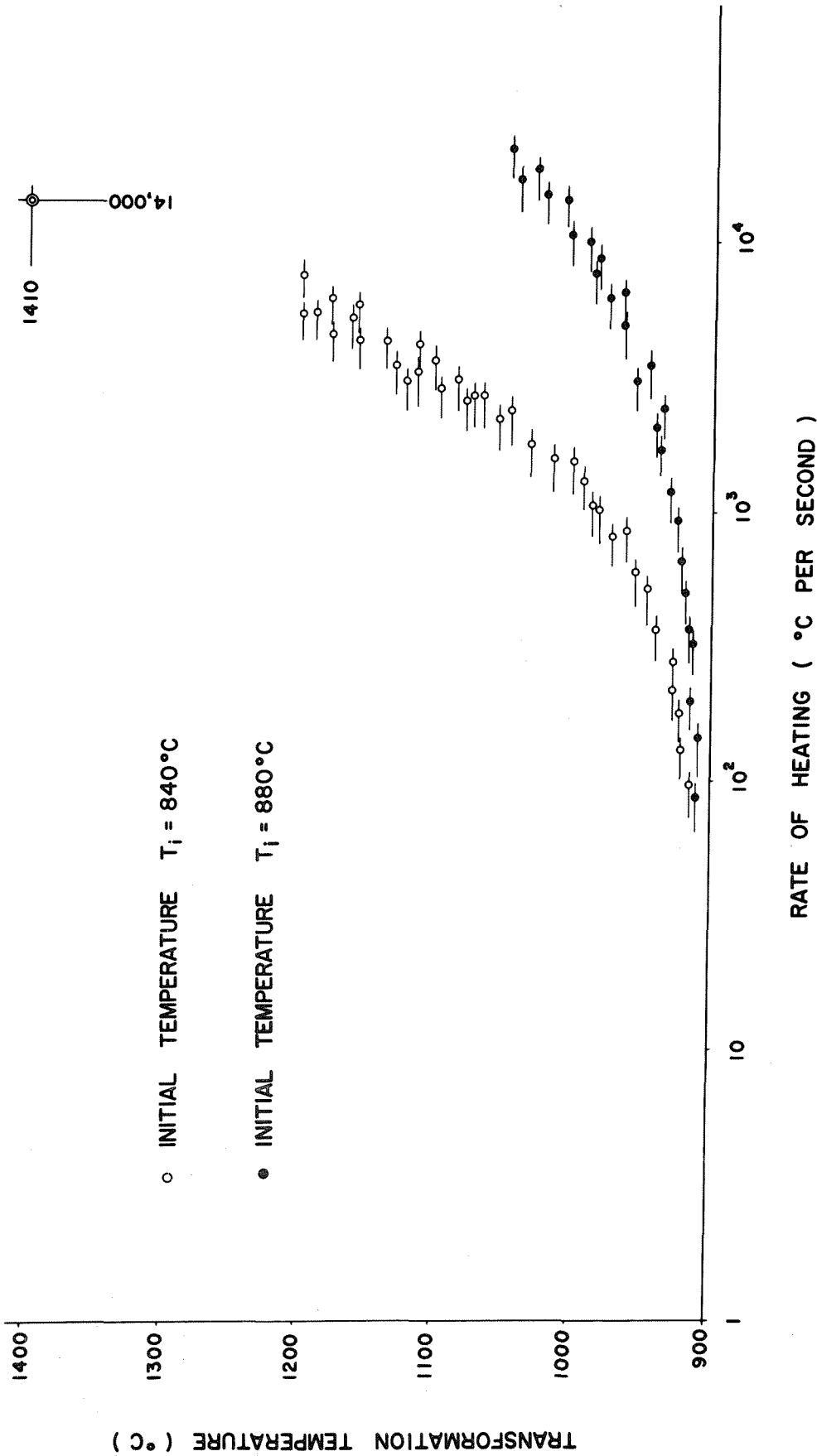


Fig. 23 - Effect of the rate of heating on the alpha to gamma transformation temperature in iron for two different initial temperatures. The point shown in the upper right corner of the diagram was not measured, but was calculated from the data obtained from the pulse heating experiments.

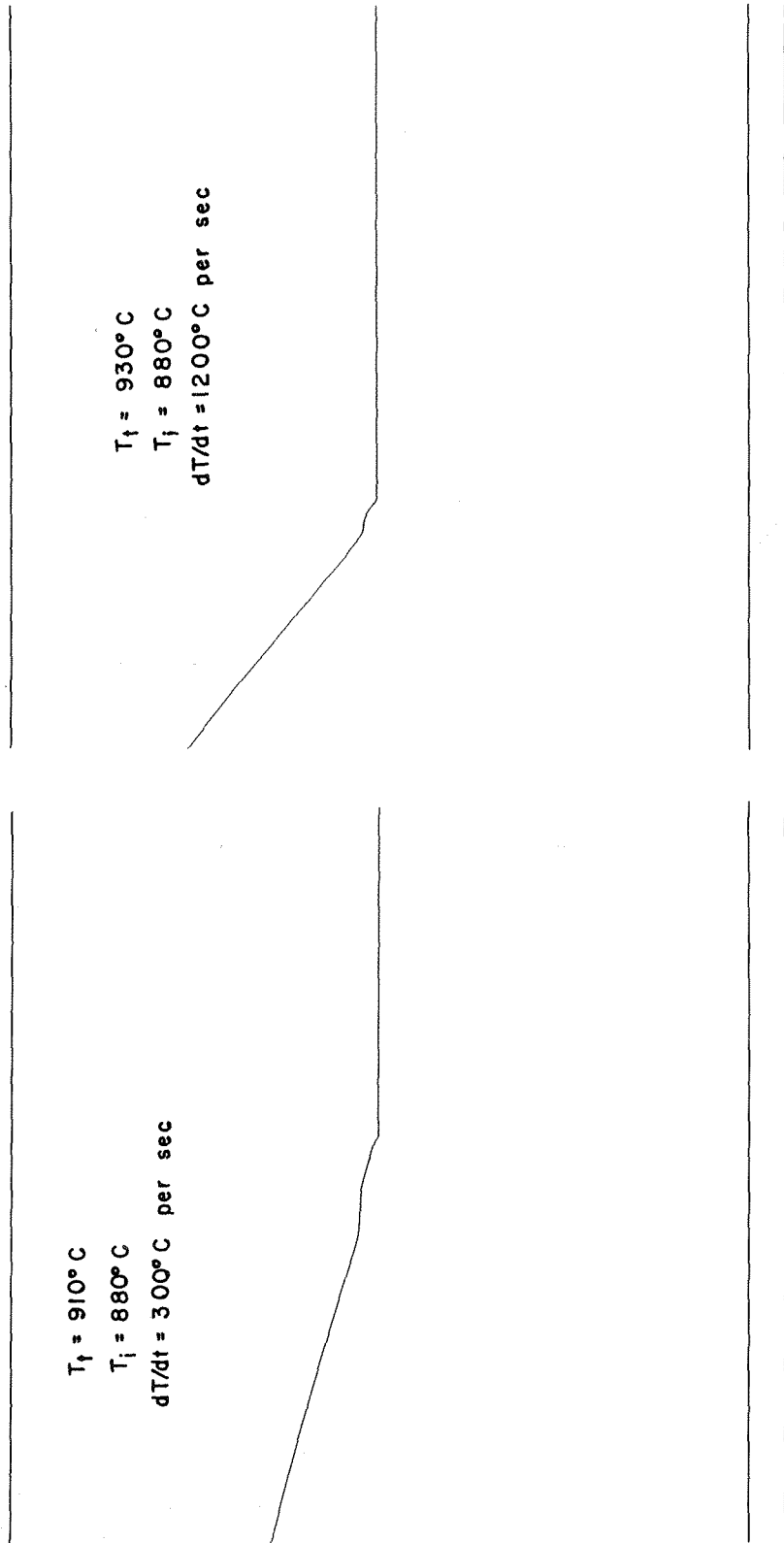


Fig. 24 - Typical records from rate of heating experiments.  
Initial temperature  $T_i = 880^\circ\text{C}$ .

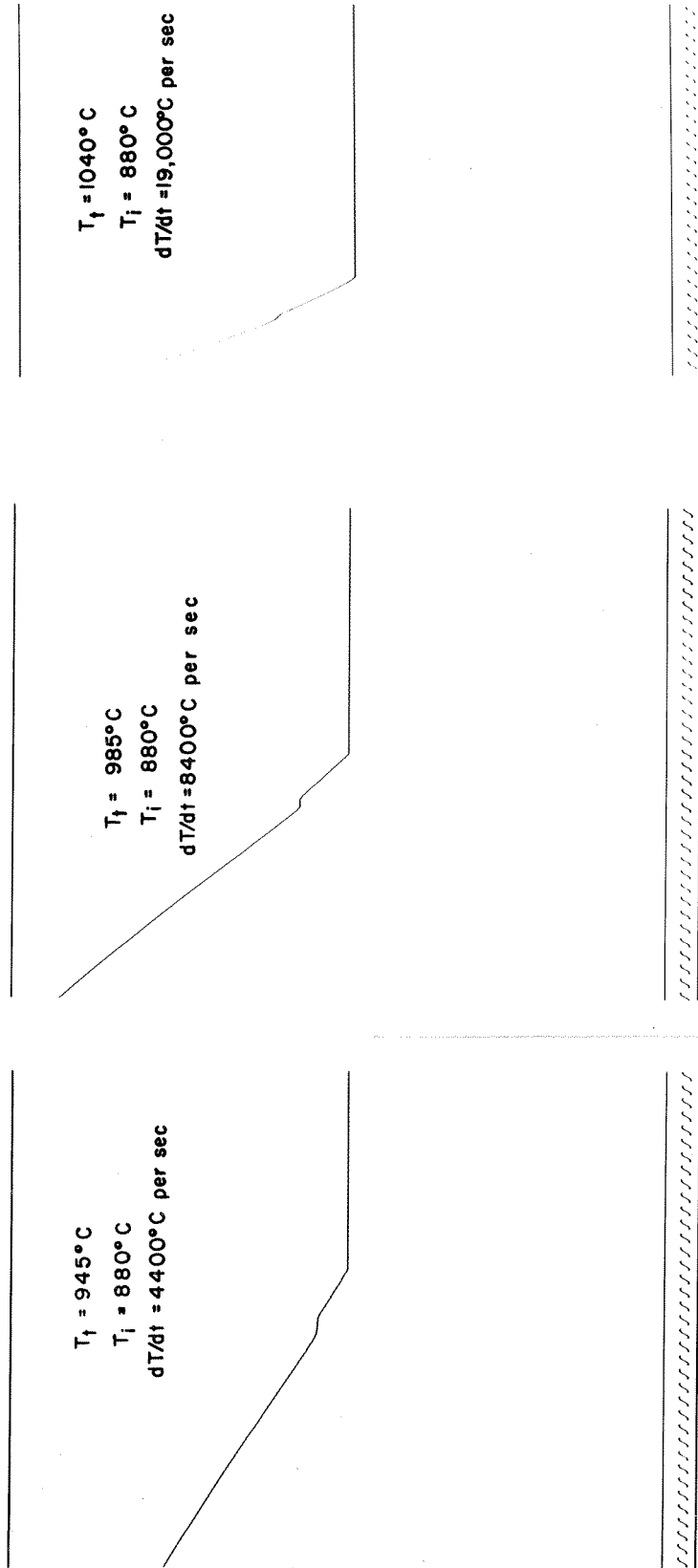


Fig. 24 - Typical records from rate of heating experiments.  
(cont.) Initial temperature  $T_i = 880$  C.

seconds. Some time after such a pulse had been applied, the transformation took place and the release of the latent heat resulted in a sudden drop of the specimen temperature. This temperature drop was immediately followed by a temperature increase bringing the specimen back to its final equilibrium temperature. Five typical oscillograph records are shown in Fig. 25. With the time scale used for these measurements (10 milliseconds = 1.35 cm on the original records) the time required to increase the specimen temperature was too short to be recorded, but has been measured from oscilloscope traces to be at about 700 microseconds. The most important measurement resulting from these experiments was the time involved between the application of the pulse and the release of latent heat. For convenience this time will be called "delay time".

About 50 experiments were performed with an initial temperature of 840 C and various final temperatures up to 1355 C. A few additional experiments were made with an initial temperature of 800 C. All the results are shown on the graph of Fig. 26, in which the difference between the observed transformation temperature and the equilibrium transformation temperature (905 C) is plotted versus the delay time. As expected, the delay time is shortened by an increase of the final specimen temperature over the equilibrium temperature. The experimental data shown in Fig. 26 seem to be contained within a scatter band indicated by the dashed lines. The uncertainty in the specimen temperature measurements was about  $\pm 5$  C and is roughly indicated by the size of the circles. The uncertainty in the determination of the

$T_f = 930^\circ\text{C}$   
 $T_i = 840^\circ\text{C}$   
 $\Delta T = 25^\circ\text{C}$   
 $\Delta t = 87 \text{ ms}$

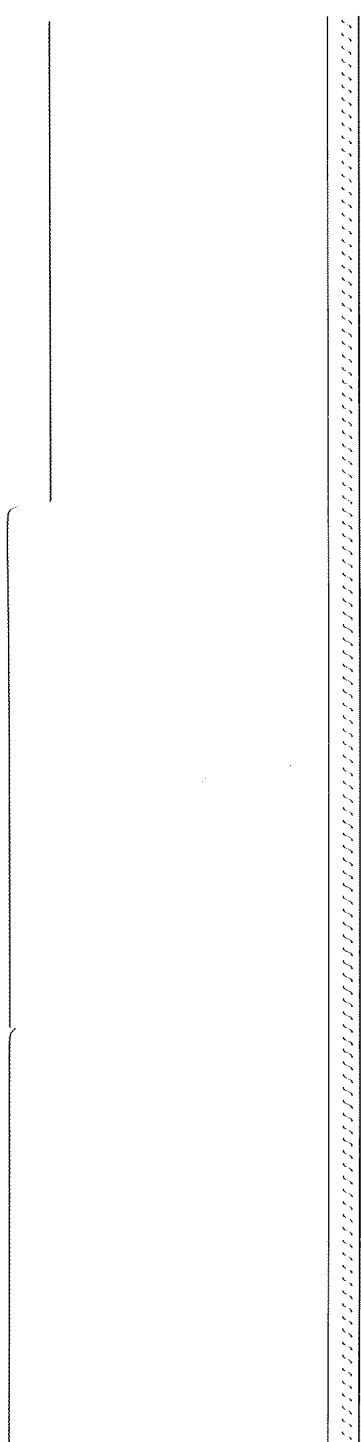


Fig. 25 - Typical record from pulse heating experiments.  
Initial temperature  $T_i = 840 \text{ C}$ .



$T_f = 1025^\circ \text{C}$   
 $T_i = 840^\circ \text{C}$   
 $\Delta T = 120^\circ \text{C}$   
 $\Delta t = 58 \text{ ms}$

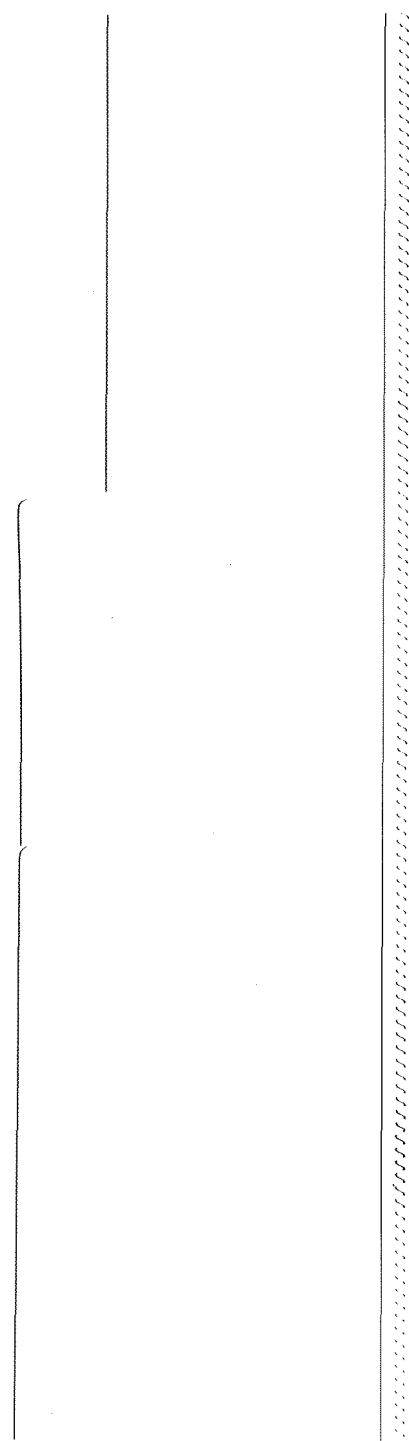


Fig. 25 - Typical record from pulse heating experiments.  
(cont.) Initial temperature  $T_i = 840^\circ \text{C}$ .

$T_f = 1140^\circ\text{C}$   
 $T_i = 840^\circ\text{C}$   
 $\Delta T = 235^\circ\text{C}$   
 $\Delta t = 33 \text{ ms}$

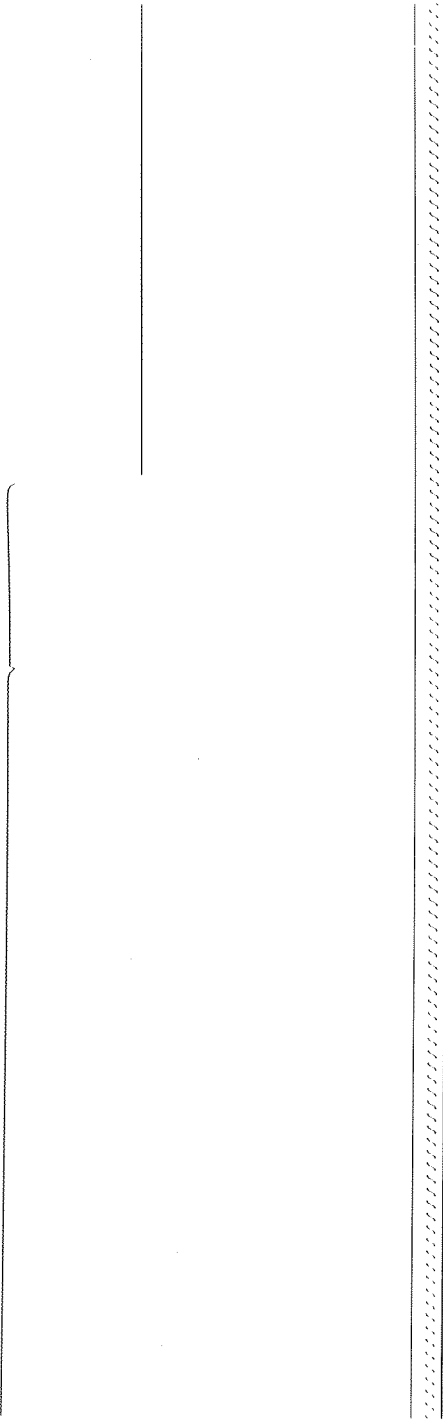


Fig. 25 - Typical record from pulse heating experiments.  
(cont.) Initial temperature  $T_i = 840 \text{ C.}$

$T_f = 1220^\circ \text{C}$   
 $T_i = 840^\circ \text{C}$   
 $\Delta T = 315^\circ \text{C}$   
 $\Delta t = 20 \text{ ms}$

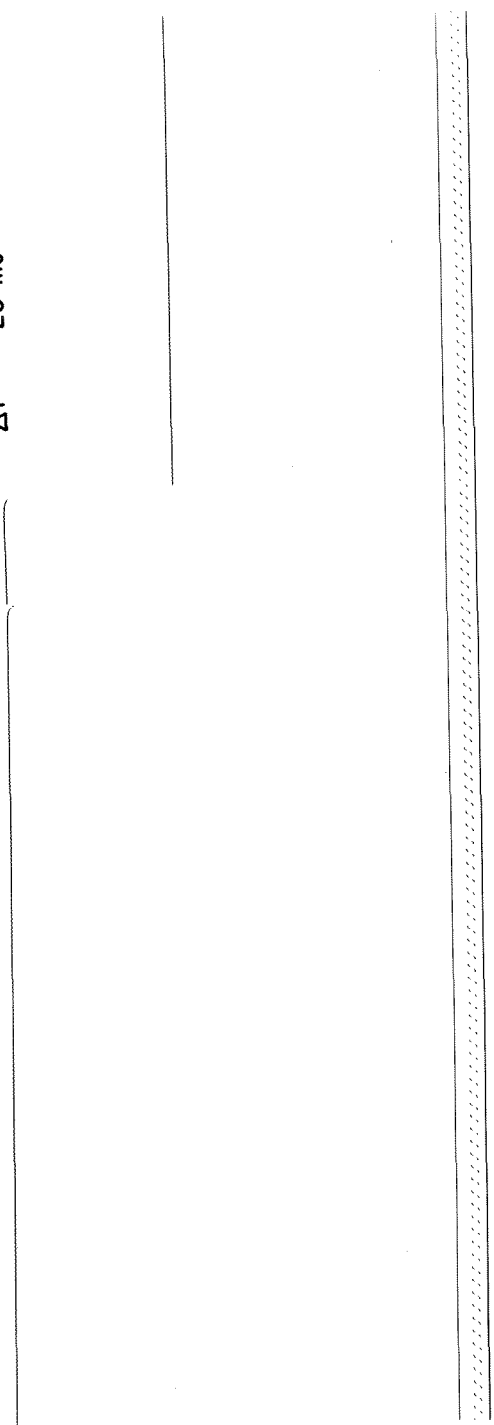


Fig. 25 - Typical record from pulse heating experiments.  
(cont.) Initial temperature  $T_i = 840^\circ \text{C}$ .

$T_f = 1355^\circ \text{C}$   
 $T_i = 840^\circ \text{C}$   
 $\Delta T = 450^\circ \text{C}$   
 $\Delta t = 10 \text{ ms}$

---

---

---

Fig. 25 - Typical record from pulse heating experiments.  
(cont.) Initial temperature  $T_i = 840 \text{ C}$ .

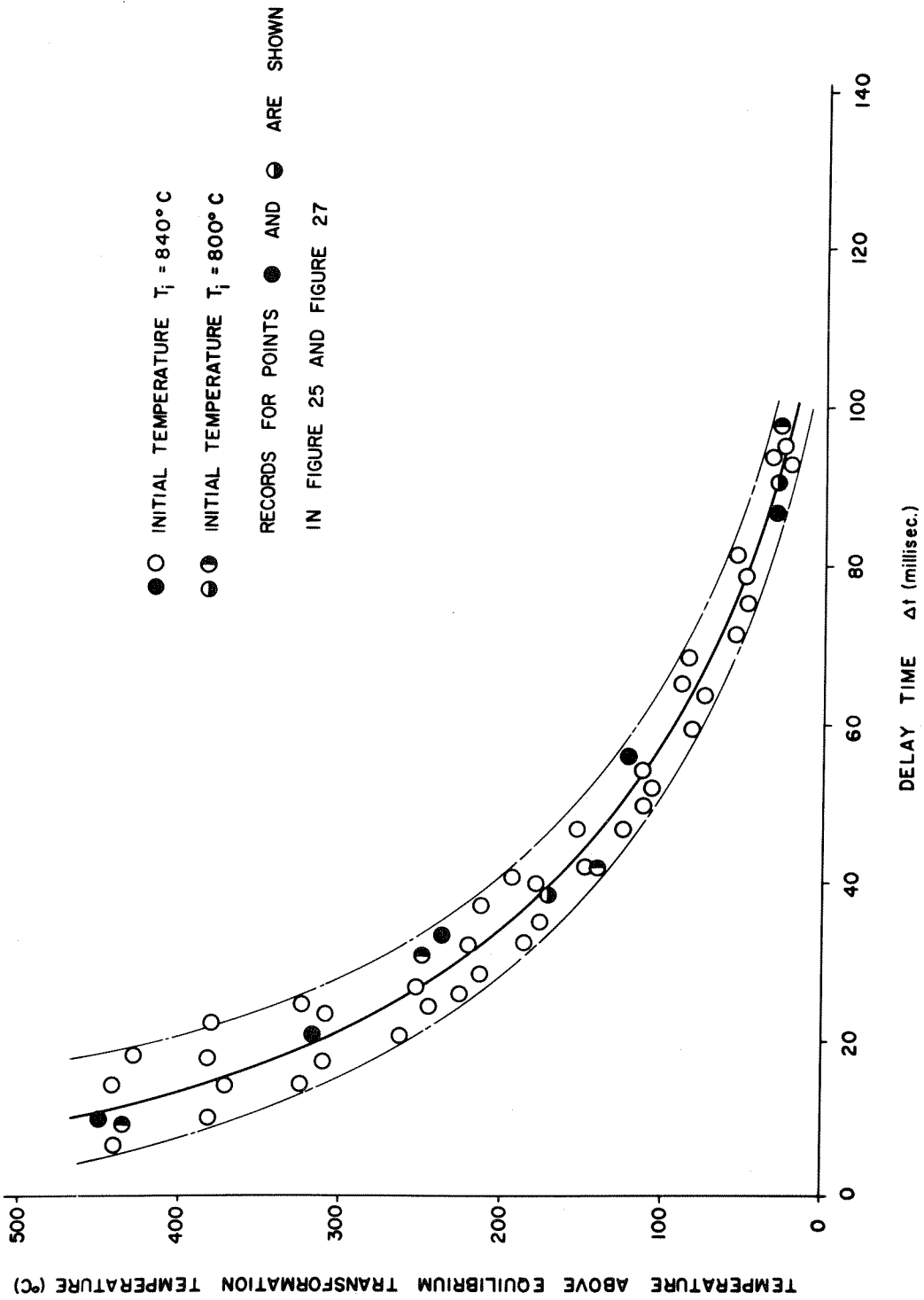


Fig. 26 - Results of pulse heating experiments showing the delay time for the alpha to gamma transformation at various temperatures.

delay time was about  $\pm 1$  milliseconds. Since the width of the scatter band shown in Fig. 26 is about  $\pm 8$  milliseconds at any temperature, it must be concluded that at least a part of the scatter in delay time measurements was due to other factors than those involved in the recording technique.

The results of the few experiments made with an initial temperature of 800 C (and shown in Fig. 27) instead of 840 C, fall at random within the limits of experimental uncertainty. Since at both 800 and 840 C the interstitial impurities are in solid solution in an all alpha iron matrix, these results are not surprising. Although it was obvious that the delay time would be affected if the initial temperature corresponded to an alpha plus gamma structure, a few experiments were made with an initial temperature of 880 C. As shown in the record reproduced in Fig. 28, a delay time was still observed, but it was only about 5 milliseconds, compared with about 80 milliseconds measured on specimens pulsed to the same final temperature but from initial temperature within the alpha field. The presence of some gamma phase in the specimen at the initial temperature obviously accelerated the transformation. All the experimental results presented in Fig. 26 are also presented in Fig. 29, in which the log of the delay time is plotted in ordinate versus the reciprocal of the temperature at which the delay time was observed. On this graph the scatter of the experimental results looks quite different from that shown in Fig. 26, because of the logarithmic delay time scale, but is still, of course, within the  $\pm 8$  milliseconds experimental uncertainty. Assuming that

$T_f = 1065^\circ\text{C}$   
 $T_i = 800^\circ\text{C}$   
 $\Delta T = 160^\circ\text{C}$   
 $\Delta t = 39 \text{ millisecond}$

$T_f = 930^\circ\text{C}$   
 $T_i = 800^\circ\text{C}$   
 $\Delta T = 25^\circ\text{C}$   
 $\Delta t = 69 \text{ millisecond}$

Fig. 27 - Typical records from pulse heating experiments.  
Initial temperature  $T_i = 800 \text{ C}$ .

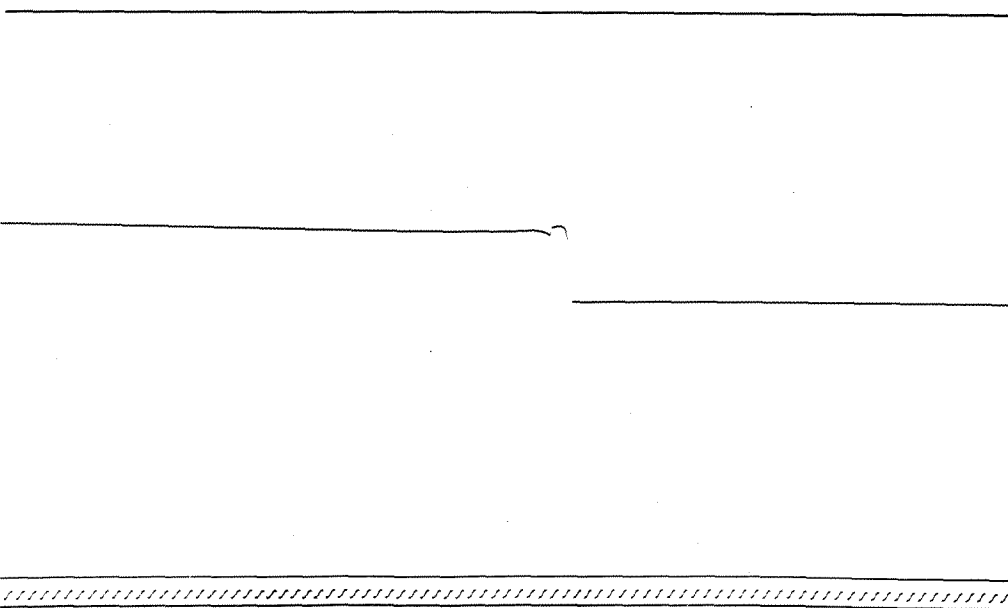
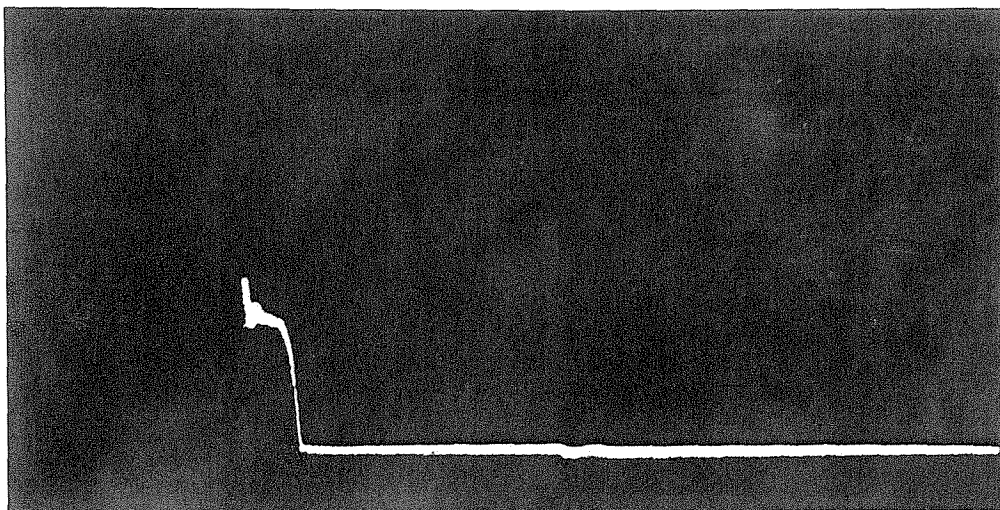


Fig. 28 - Typical records from pulse heating experiments. Initial temperature  $T_i = 880$  C. The upper record was obtained with the oscilloscope and the bottom one is the oscillograph trace obtained in the same experiment.



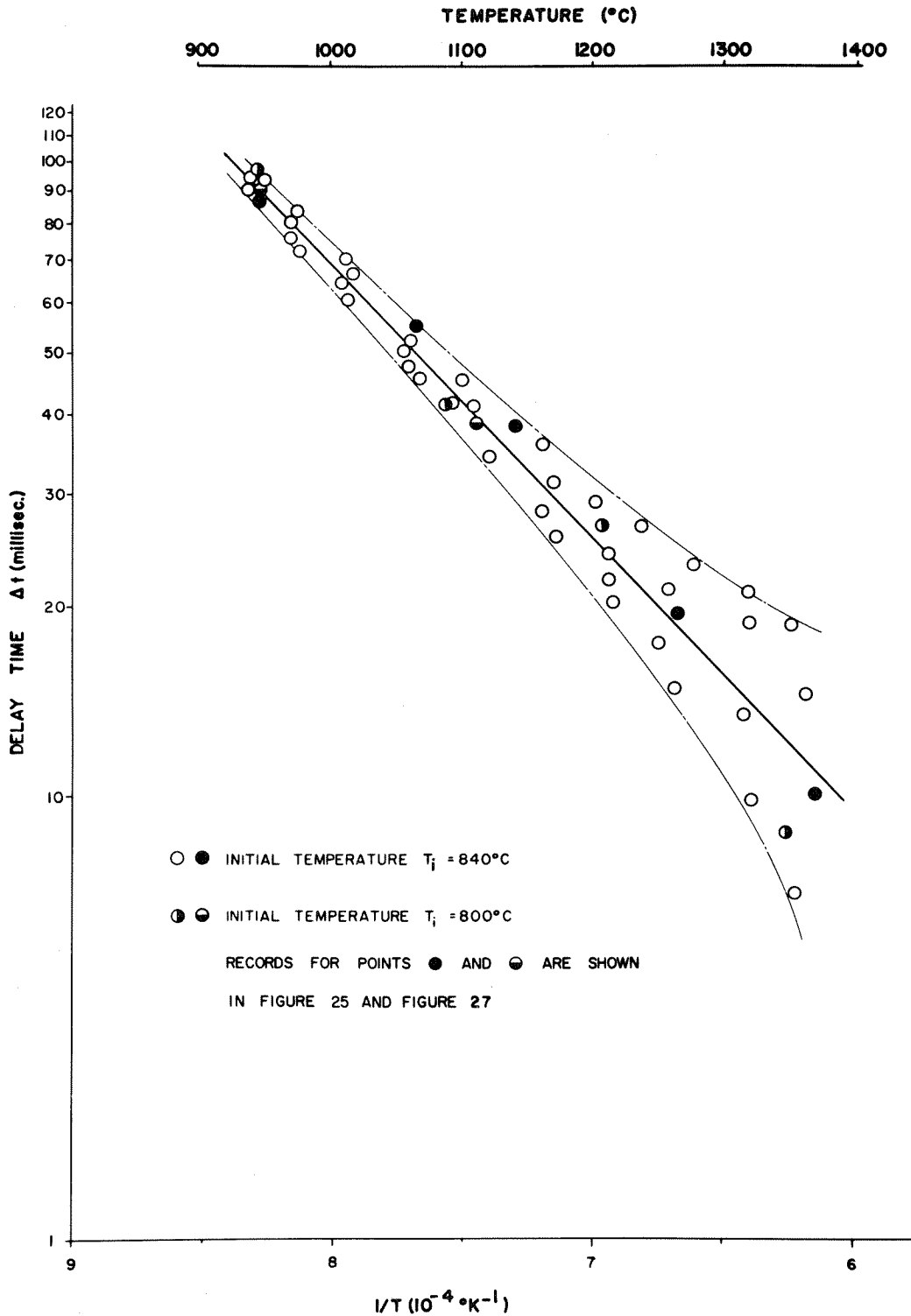


Fig. 29 - Results of pulse heating experiments (same as those shown in Fig. 26) plotted on log of delay time versus reciprocal of absolute temperature scales.

the delay time process in the transformation from alpha to gamma iron is governed by a heat of activation, the experimental results shown in this figure should fall on a straight line. The solid line, shown in Fig. 29, was determined as the best fit, taking into account the  $\pm 8$  milliseconds uncertainty in the delay time measurements. The resulting heat of activation was computed to be  $20,500 \pm 1,400$  calories per mole ( $1.17 \pm 0.08$  ev per atom).

Delay time measurements were obviously limited to a range of temperatures within which the gamma phase is stable (from about 905 to 1410 C). By extrapolating the results shown in Fig. 29, it may be concluded that the delay time near 905 C would be somewhere between 100 and 120 milliseconds, and the delay time near 1410 C would be in the range of 3 to 18 milliseconds. Since it was possible to bring the specimen temperature from 840 C to a temperature above 1410 C in less than 3 milliseconds (namely about 700 microseconds), it was anticipated that in such experiments no transformation should occur. A typical record of a test in which the temperature of the specimen was increased from 840 C to 1425 C in 700 microseconds (rate of heating of about 840,000 C per second) is shown in Fig. 30 and, as expected, no latent heat of transformation was observed. It is therefore established that the gamma iron structure can be suppressed by fast enough heating from the alpha to the delta field.

### C. Correlation between Rate of Heating and Pulse Heating Experiments.

From the results obtained in pulse heating experiments, leading

$T_f = 1425^\circ\text{C}$   
 $T_i = 840^\circ\text{C}$   
 $\Delta T = 520^\circ\text{C}$

The figure area is mostly blank, with a few faint horizontal lines and a vertical line on the right side, possibly representing a recording artifact or a separator line.

Fig. 30 - Typical record demonstrating passage from alpha to delta iron without transformation into the gamma phase.

to a unique relationship between the time required to complete the transformation and the temperature, it should be possible to determine the effect of rate of heating on the transformation temperature. If the rate of heating is constant, it may be assumed that the time required to reach a given transformation temperature is an "average" delay time. If  $t_d$  denotes the delay time corresponding to a temperature  $T_f$ , the "average" delay time  $t_x$  at which the transformation will take place at the temperature  $T_f$  under constant rate of heating is given by

$$t_x = \frac{\int_{T_c}^{T_f} C e^{Q/RT} dT}{T_o - T_c} \quad (\text{IV-I})$$

in which  $T_c$  is the critical temperature (905 C) under equilibrium conditions. The value of  $t_x$  may be obtained by graphical integration as shown in Fig. 31. This graph shows the delay time versus the temperature. The time  $t_x$ , corresponding to a delay time  $t_d$  at a temperature  $T_o$  is such that the two shaded areas on the graph are equal. Once  $t_x$  has been determined, the corresponding rate of heating is given by the slope (angle  $\alpha$ ) of the straight line joining  $T_c$  to  $t_x$ . This method was applied to the results obtained in the present study. The relationship between transformation temperature and delay time was assumed to be that shown by the solid line in Fig. 26. After the graphical integration, described above, was performed, the transformation temperature was obtained as a function of rate of heating.

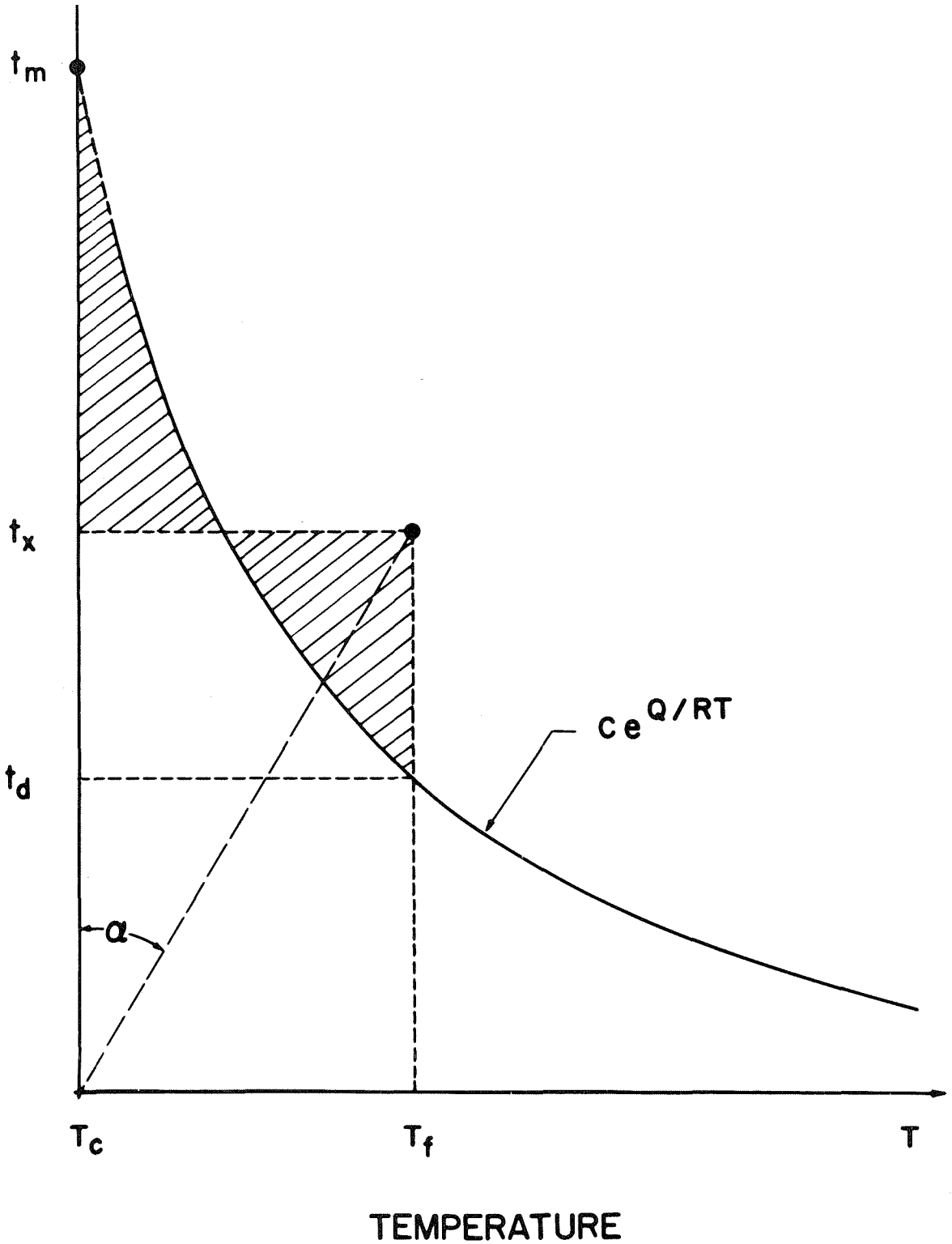


Fig. 31 - Diagram demonstrating the method used for correlating the results of pulse heating and rate of heating experiments.

A plot of this function is shown in Fig. 32 as curve B. In the same figure, curve A represents the experimental results obtained in the rate of heating experiments. It is quite apparent that the slight shift between the two curves is not significant, considering the scatter in the measurements shown in Fig. 23 and Fig. 26.

It is therefore concluded that the results of rate of heating experiments can be deduced from the basic relationship between delay time and temperature obtained from pulse heating experiments. It might be interesting to point out that, from rate of heating measurements, it is not possible to obtain a relationship between delay time and temperature. It is indeed impossible to use equation (IV-I) in this case, since the function  $C e^{Q/RT}$  cannot be evaluated from data obtained from rate of heating experiments.

The result mentioned in section A of this chapter, concerning the absence of observable latent heat of transformation for rates of heating greater than about 8000 C per second, will now be discussed. It is obvious that no transformation from alpha to gamma will take place if the rate of heating is greater than a certain critical rate. This critical rate can be estimated by using the graphical method described above and applying it to a final temperature of 1410 C (transformation temperature gamma to delta). This operation was carried out and the critical heating rate for by-passing the gamma phase was determined to be approximately 14,000 C per second. This critical rate is greater than 8000 C per second, above which no transformation was detected. It should be pointed out, however, that at

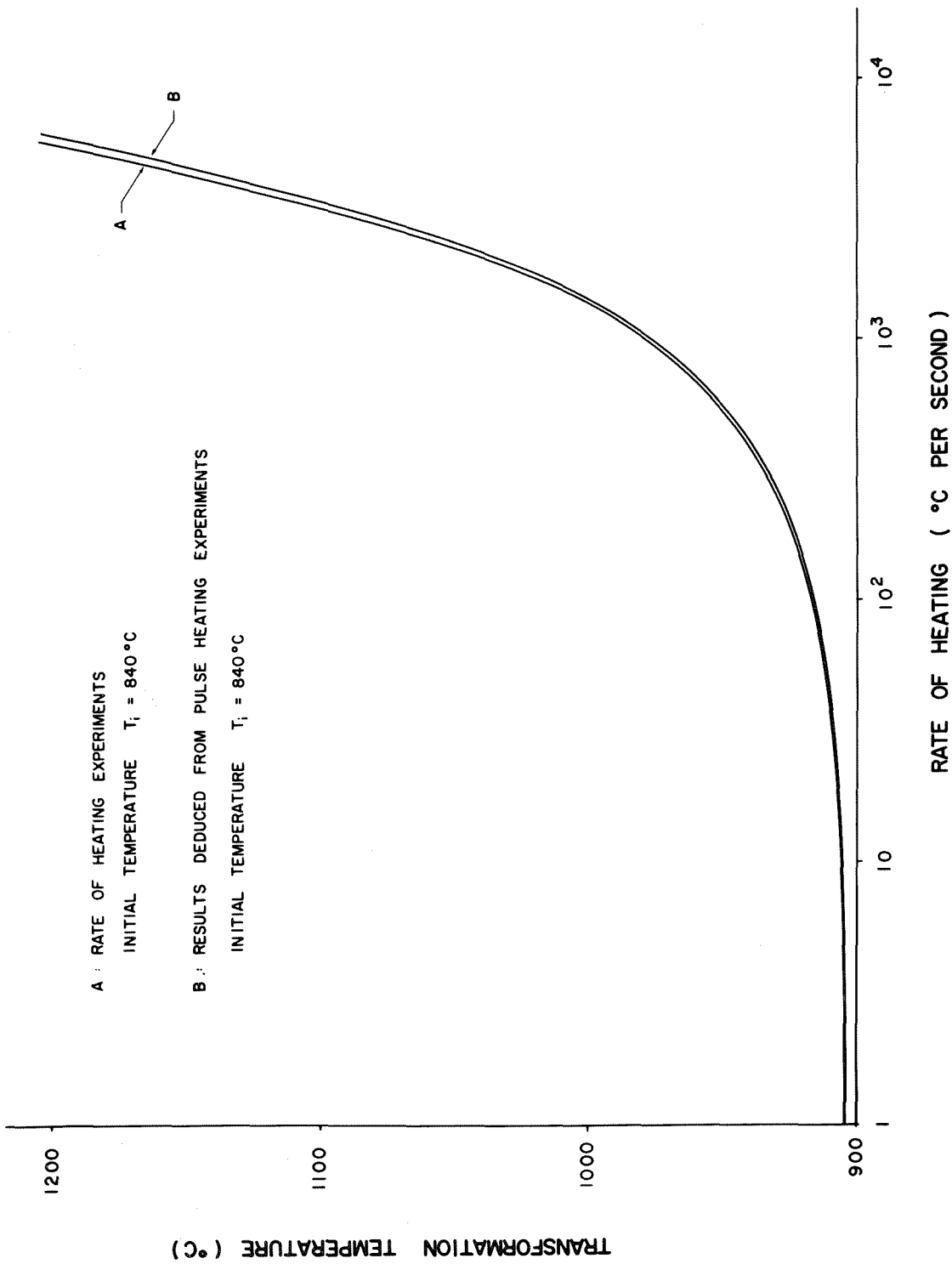


Fig. 32 - Experimental curve of transformation temperature versus rate of heating (A) and calculated curve (B) deduced from the pulse heating experiments.

rates approaching 8000 C per second, the detection of the latent heat of transformation became very difficult because of limitation of the recording equipment. It is also pertinent to point out that, as a consequence of the lack in sensitivity of the equipment, the highest transformation temperature recorded in the rate of heating experiments was 1200 C (see Fig. 23) which is some 200 C below the gamma to delta transformation temperature. Within the limits of experimental scatter, shown in Fig. 23, a smooth curve traced through the data point can be extrapolated in such a manner as to pass through a point corresponding to a heating rate of 14,000 C per second and a temperature of 1410 C. The experimental rate of heating results are, therefore, compatible with the critical rate of heating deduced from delay time measurements.

---



## V. DISCUSSION OF RESULTS

The experimental proof for the existence of a delay time in the transformation of iron from the alpha to the gamma phase is the most significant result presented in this thesis. Although such a delay time was anticipated it had never been measured by previous investigators.

The delay time may be defined as the time it takes for completing the transformation from the alpha to the gamma phase at a given temperature within the range of stability of the gamma phase. As explained in section E of Chapter III, the time required to increase the temperature of the specimen from the alpha to the gamma field was short (about 700 microseconds) compared with the time necessary for completion of the transformation (about 8 milliseconds) and the transformation took place under essentially isothermal conditions. The delay time observed under these conditions is therefore a function of the temperature only and it was found that the time-temperature relationship obeys an Arrhenius type equation with a heat of activation of 20,500 cal per mole (1.17 ev. per atom). Several different atomic mechanisms could probably lead to a satisfactory explanation of the results obtained in this investigation. The following discussion describes a possible atomic process by which the delay time can be explained, at least qualitatively.

It was first assumed that the alpha to gamma allotropy of iron is somewhat similar to the transformation of austenite to martensite.

Since it took about 700 microseconds to increase the temperature from its initial value in the alpha range to its final value in the gamma range, it may be assumed that gamma nuclei were generated during this time. While the specimen was being kept at constant temperature in the gamma range, the number of gamma nuclei did not change appreciably but their size increased at a certain rate. When a certain critical size was reached, the transformation proceeded catastrophically through a shear mechanism. At that time, the latent heat of transformation, or at least a large fraction of this heat, was suddenly released, as shown in the experiments. Following the assumption that all the gamma nuclei were formed within an extremely short time after the final temperature had been reached, the delay time would be directly connected to the rate of growth of the nuclei to a critical size required for the initiation of the shear transformation. This mechanism is compatible with the fact that the delay time is related to the temperature by a rate equation of the Arrhenius type. In this suggested mechanism, the rate at which new gamma nuclei are produced while the specimen is maintained at its final temperature, has no direct influence on the delay time. This means that the shear transformation is made possible when a relatively small number of nuclei have reached the critical size (through a diffusion process) and the total number nuclei of sub-critical size present in the matrix at that time has no effect on the initiation of the shear transformation.

From the relationship between delay time and temperature established experimentally, it was found that the heat of activation

connected with the alpha to gamma kinetics was  $20,500 \pm 1400$  cal per mole. If the mechanism of transformation just described is accepted, the heat of activation should correspond to the diffusion process taking place during the isothermal growth of the alpha nuclei, up to their critical size. In really pure iron, this heat of activation should be very close to that found for self-diffusion in alpha iron (about 57,200 cal per mole <sup>(25)</sup>). It was clearly pointed out in Chapter I that the present investigation was not made with pure iron, but with an iron-carbon-nitrogen alloy. Although the carbon and nitrogen concentrations appear to be small when given in parts per million, they are actually quite appreciable on an atomic scale. In fact, the iron used in these experiments contained one carbon atom in a cube built on an edge corresponding to 11.8 unit cells of iron, and one nitrogen atom was present in a cube built on only 8.1 unit cells. It is therefore obvious that the local concentrations of carbon and nitrogen can be greatly increased by migration of these two interstitial atoms through relatively short distances. Since both carbon and nitrogen have a very marked tendency to stabilize the gamma phase of iron, the rate of growth of the gamma nuclei is greatly enhanced by the presence of carbon and nitrogen. As a consequence, the diffusion rates of carbon and nitrogen through the iron lattice become the dominant factor controlling the rate of growth of the gamma nuclei. The fact that the heat of activation measured in the delay time experiments is close to that reported for both carbon and nitrogen diffusion (20,500 cal per mole compared with 20,100 cal per mole for carbon <sup>(25)</sup> and 17,700 cal

per mole for nitrogen <sup>(26)</sup> , is compatible with the proposed explanation of a delay time based on the growth of gamma nuclei controlled by the diffusion of carbon and nitrogen through the iron matrix.

---

## VI CONCLUSIONS

In order to avoid any confusion between experimental facts and their theoretical interpretation, the conclusions will be given in two separate sections.

### A. Experimental Facts

When a specimen of iron (containing a certain amount of carbon and nitrogen) is suddenly heated (within less than 700 microseconds) from an initial temperature in the alpha phase (800 or 840 C) into a final temperature within the gamma phase (between 910 and 1400 C), the bulk of the allotropic transformation, detected by a sudden release of the latent heat, takes place a certain time after the final temperature has been reached. The relationship between this delay time and the final temperature follows a Arrhenius type rate equation with a heat of activation of  $20,500 \pm 1400$  cal per mole. When the final temperature is above the gamma to delta iron transformation (1410 C), the specimen can be heated from alpha to delta iron without going through the gamma phase. The effect of the rate of heating on the measured alpha to gamma transformation temperatures can be quantitatively explained from the measurements of the delay time.

## B. Interpretation

The preceding experimental facts were interpreted as follows. As soon as the specimen temperature is above the alpha to gamma equilibrium temperature, a large number of nuclei of the gamma phase are present. These nuclei, however, must reach a certain critical size before a very fast shear transformation from alpha to gamma can take place and the growth of these nuclei to their critical size is controlled by a diffusion process. In the present case of iron containing carbon and nitrogen, the diffusion of these two interstitial atoms rather than the self diffusion of iron control the diffusion rate, and hence, the heat of activation determined experimentally for the delay time is very close to the heat of activation generally accepted for diffusion of carbon and nitrogen in alpha iron.

---

REFERENCES

- (1) Tisza, L: "On the General Theory of Phase Transformation", "Phase Transformation in Solids", Wiley, New York, (1951), p. 1-37
- (2) Seitz, OF: "Fundamental Aspects of Diffusion in Solids", "Phase Transformation in Solids", Wiley, New York, (1951), p. 77-148
- (3) Smoluchowsky, R: "Nucleation Theory", "Phase Transformations in Solids", Wiley, New York, (1951), p. 149-182
- (4) Barrett, C: "Transformations in Pure Metals", "Phase Transformations in Solids", Wiley, New York, (1951), p. 343-365
- (5) Mayer, J. E.: "A General Method for Imperfect Crystals and Phase Transitions", "Phase Transformation in Solids", Wiley, New York, (1951), p. 38-66
- (6) Cohen, M: "The Martensite Transformation", "Phase Transformations in Solids", Wiley, New York, (1951), p. 588-660
- (7) Hardy, H. K. and T. J. Heal: "Nucleation-and-Growth Processes in Metals and Alloys", "The Mechanism of Phase Transformations in Metals", The Institute of Metals, London, (1956), p. 1-46
- (8) Cohen, M., E. S. Machlin and V. G. Paraujpe: "Thermodynamics of the Martensite Transformation in Thermodynamics in Physical Metallurgy", ASM, Cleveland, Ohio, (1950), p. 242-270
- (9) Cohen, M: "Nucleation of Solid State Transformation", AIME Trans. Vol. 212, (1958), p. 171-183
- (10) Richman, M. H., M. Cohen and H. G. F. Wilsdorf: "Experimental Evidence for Martensite Embryos", Acta Met. Vol. 7, (1959), p. 819-820
- (11) Jawson, M. A.: 3rd International Congress Cryst. Paris, (1954)
- (12) Geisler, A. H.: "Crystallography of Phase Transformations", Acta Met. Vol. 1, (1953), p. 260-281
- (13) Eichen E., and J. W. Spretnak: "The Mechanism of the Allotropic Transformation in High Purity Iron", Trans. ASM, Vol. 51, (1959), p. 454-475

- (14) Esser, H., W. Eilender and E. Speule: "Das Haertungsschaubild der Eisen-kohlenstoff-Legierungen", "Archiv fuer das Eisen-huettenwesen", Vol. 6, (1933), p. 389
- (15) Duwez, P: "Effect of Rate of Cooling on the Alpha-Beta Transformation in Titanium and Titanium-Molybdenum Alloys", Trans. AIME, Vol. 191, (1951), p. 765-771
- (16) Greninger, A. B.: "The Martensite Thermal Arrest in Iron - Carbon Alloys and Plain Carbon Steels, Trans. ASM, Vol. 30, (1942), p. 1-26
- (17) Duwez, P: "The Allotropic Transformation of Hafnium", J. of Appl. Phys., Vol. 22, No. 9, (1951), p. 1174-1175
- (18) Duwez, P: "The Effect of the Rate of Cooling on the Allotropic Transformation Temperature of Uranium", J. of Appl. Phys., Vol. 24, No. 2, (1953), p. 152-156
- (19) Chace, W. G., and H. K. Moore: "Exploding Wires", Plenum Press, New York, (1959)
- (20) Low, J. R., and M. Gensamer: "Aging and the Yield Point in Steel", Trans. AIME, Vol. 158, (1944), p. 207-218
- (21) Glasoe, G. N. and J. V. Lebacqz: "Pulse Generators", MIT Radiation Laboratories Series, Vol. 5, McGraw-Hill, New York, (1948)
- (22) LePage, W. R., and S. Seely: "General Network Analysis", McGraw-Hill, New York, (1952)
- (23) Millman, J., and H. Taub: "Pulse and Digital Circuits", McGraw-Hill, New York, (1956)
- (24) Thomason, J. G.: "Linear Feedback Analysis", Pergamon Press, New York, (1956)
- (25) Buffington, F. S., K. Hirano, and M. Cohen: Private Communication; will be published in Acta Met.
- (26) Wert, C., and C. Zener: Phys. Rev. 76, (1949), p. 1169-1175



APPENDIXApproximate calculation of the skin-depth in the pulse heated specimen.

The skin-depth, due to the high frequency components of the voltage pulse, can be obtained from the equation

$$\delta = \sqrt{\frac{2}{\omega \sigma \mu}} \quad (A-1)$$

where  $\omega$  is the maximum angular frequency,  $\sigma$  the electrical conductivity, and  $\mu$  the permeability of iron.

The maximum angular frequency of a circuit containing a capacitor, an inductor, and a resistor in series is given by

$$\omega = \frac{(2\pi)^2}{\sqrt{LC}} \quad (A-2)$$

where C is the capacitance and L is the inductance of the circuit. The upper limit of the angular frequency of the transmission line circuit can also be obtained from equation A-2,\* . With a capacitance C of 28 microfarad and a inductance L of 0.05 millihenry of the last section, the maximum angular frequency is then

$$\omega = \frac{(2\pi)^2}{\sqrt{LC}} = \frac{4\pi^2}{\sqrt{0.05 \cdot 10^{-3} \cdot 28 \cdot 10^{-6}}} = 1.06 \cdot 10^6 \text{ rad per sec}$$

The electrical conductivity of iron at 1000 C is approximately 1 per micro ohm-meter (from "Metals Handbook", American Society of Metals, Cleveland, Ohio (1948)).

\* Assuming that only the last section of the line is important for the determination of this frequency.

The permeability of iron above the curie temperature is very near to that of free space (from Bozarth, R.M.: "Ferro-magnetism," Van Nostrand, New York 1959). The permeability of iron at 1000 C is therefore taken to  $4\pi \cdot 10^{-7}$  henry per meter.

The skin-depth of the specimen is then

$$\delta = \sqrt{\frac{2}{\omega \sigma \mu}} = \sqrt{\frac{2}{1.06 \cdot 10^6 \cdot 10^6 \cdot 4\pi \cdot 10^{-7}}} = 1.22 \cdot 10^{-3} \text{ meter}$$

or  $\delta = \underline{1.22 \text{ mm}}$

---